On the Capacity of Point-to-Point and Multiple-Access Molecular Communications With Ligand-Receptors

Gholamali Aminian, Maryam Farahnak-Ghazani, Mahtab Mirmohseni, *Member, IEEE*, Masoumeh Nasiri-Kenari, and Faramarz Fekri, *Fellow, IEEE*

***Abstract*—In this paper, we consider bacterial point-to-point and multiple-access molecular communications with ligand-receptors. For point-to-point communication, we investigate common signaling methods, namely, the level scenario, in which the information is encoded into multiple concentration levels of a single molecule type, and the type scenario, in which the information bits are encoded in multiple molecule types each with a single concentration level. We investigate the tradeoffs in the two scenarios in terms of the capacity. We derive an upper bound on the capacity using a Binomial channel model and the symmetrized Kullback–Leibler divergence. A lower bound is also derived when the environmental noise is negligible. We also consider the blocking effect of a receptor by a different molecule type. Finally, we study multiple-access communications, for which we investigate three scenarios based on molecule and receptor types: 1) same molecule types with different labeling and the same receptor types; 2) different molecule types with different receptor types; and 3) the same molecule types with the same receptor types. We investigate the tradeoffs in the three scenarios in terms of the total capacity. We derive inner bounds on the capacity region of these scenarios when the environmental noise is negligible.**

***Index Terms*—Multiple-access molecular communication, binomial channel capacity, receptor Markov modeling.**

I. Introduction

MOLECULAR communication (MC) has stimulated a great deal of interest because of its potentially broad applications. It is a bio-inspired method that enables communication in nano-micro scale environments. An MC system relies on molecules to transport the information and is comprised of transmission process, channel, and reception process. The transmitter may encode information into the concentration, type, or releasing time of the molecules. For instance in [1] and [2], modulation techniques based on using multiple molecule types are presented. In [3], an on-off keying modulation is proposed where molecules are released only when the information bit is one. For an MC channel, different mechanisms are introduced, among which diffusion process is the most favorable, as it does not require any prior infrastructure. Different models have been proposed for diffusion-based molecular communication channels. While in this medium, each individual molecule propagates randomly and independently via Brownian motion, for the high number of the released molecules, a deterministic model can be used by neglecting the diffusion noise. As such, the channel input-output is described by a differential equation according the Fick's law of diffusion. In fact, the deterministic model reflects the average behavior of the channel. There are two reception models for an MC receiver. The first model is a perfect absorber where the receiver absorbs the hitting molecule. The second, which is more realistic, is the ligand-receptor binding receiver, where the hitting molecule is absorbed by the receptor with some binding probability [4], [5].

To understand the fundamental limits of MC, one has to investigate the maximum achievable rate, i.e., the capacity, of these systems. One of the first papers to address the need for an information theoretic analysis of MC systems is [6]. In [7]–[9], the authors study the achievable information rates in MC for a timing channel. In [3], [4], and [10]–[14], the authors consider transmission strategies (binary or quaternary) for diffusion-based MC and analyze the achievable information rates. For an on-off keying modulation, it is shown in [3] that if there is no interference from the previous transmission slots and no environmental noise,[1] the channel can be modeled by a Z-channel and the capacity can be computed accordingly. Intersymbol Interference (ISI) is considered in some of the works on the MC capacity [12], [15], [16]. In [12], by modeling the ISI with a two states Markov chain, an achievable rate is computed. In [15], the capacity of diffusion-based MC is studied under a deterministic channel model taking into account the ISI. In [16], the upper and lower bounds under a Poisson channel model for an MC system with memory are computed. The above papers focus on the MC channel, while the MC capacity analysis should also include the reception

Manuscript received September 18, 2015; revised February 26, 2016 and May 18, 2016; accepted May 25, 2016. Date of publication June 6, 2016; date of current version August 2, 2016. This work has been supported in parts by INSF Research Grant on "Nano-Network Communications." The work of F. Fekri was supported by the National Science Foundation under Grant CNS-111094. This paper has been presented in part at the IEEE International Symposium on Information Theory, Wan Chai, Hong Kong, June 2015. The associate editor coordinating the review of this paper and approving it for publication was S. M. Moser.

G. Aminian, M. Farahnak-Ghazani, M. Mirmohseni, and M. Nasiri-Kenari are with the Sharif University of Technology, Tehran 11155-4363, Iran (e-mail: aminian@ee.sharif.ir; farahnakghazani_maryam@ee.sharif.ir; mirmohseni@sharif.edu; mnasiri@sharif.edu).

F. Fekri is with the Georgia Institute of Technology, Atlanta, GA 30332-0250 USA (e-mail: faramarz.fekri@ece.gatech.edu).

Digital Object Identifier 10.1109/TMBMC.2016.2577019

[1] Environmental noise is caused by the existence of the same molecule types from other sources in the environment. These sources are explained in [25].

process. Ligand-receptors are modeled by a Markov chain in [4], by a discrete-time Markov model in [10], and by a Binomial Channel (BIC) for a bacterial colony in [17]. The randomness in the ligand-receptor binding process is modeled in [18]. In this paper, we study a ligand-receptor that is modeled by a BIC and provide a capacity analysis of bacteria based point-to-point and multiple-access MC systems [17]. We consider a deterministic model for the diffusion channel.

The BIC is defined by $P(y|x) = \binom{q}{y} x^y (1-x)^{q-y}$ where the input is $x \in [0, 1]$, the output is $y \in \{0, 1, \ldots, q\}$ and q is a given natural number which shows the number of trials. Moreover, average and peak constraints on the input x may exist. The works on the BIC capacity mostly exploit one of the following approaches. The first approach is to approximate the BIC with a Gaussian channel with an input-dependent noise [17], [19]. The capacity of a Gaussian channel with an input-dependent noise is computed numerically in [17], and upper and lower bounds on its capacity are derived in [19]. The second approach is to study the BIC capacity without approximation. It is shown in [20] from the dual viewpoint of universal encoding of a discrete memoryless Bernoulli source and for large values of q that asymptotic minimax redundancy for universal encoding behaves like $\frac{1}{2}\log\frac{q}{2\pi e} + \log\pi$. However, there is no explicit formula for BIC capacity and even no explicit upper or lower bounds on the BIC capacity when q is not large enough. An algorithm to compute the BIC capacity has been presented in [21], using convex optimization methods. Since the ligand-receptor process is modeled as a BIC, to consider the channel ISI effect in a ligand-receptor based MC system, one has to deal with the capacity of BIC with memory. The capacity achieving distributions for BIC with memory are studied in [22]. Unfortunately, the BIC capacity even without memory is still an open problem and, to the best of our knowledge, there is no work on the information theoretic analysis of a BIC with memory. To gain some insight on the problem, we consider a more tractable model and study the capacity of ligand-receptor process based on a BIC without memory. That is, we assume a diffusion based MC without ISI. As shown in [16], the capacity of channels without memory provides an upper bound on the capacity of channels with memory, which makes our upper bound result an upper performance limit for the case with ISI. In addition, some ISI mitigation techniques have been proposed [23]–[25], which may be used in practice to reduce the ISI in channel. Particularly, in [25], the use of enzymes for reducing the chemicals that remain in the channel from previous transmissions is proposed. Though the ISI cannot be entirely canceled in a practical scenario, its remaining effect can be negligible. This supports our memoryless (ISI-free) assumption.

The bacteria based point-to point communication system is first introduced in [17], and its extension to multiple-access communication have been studied in [26]–[28] for a diffusion channel and ligand-receptors, where the transmitters use binary on-off keying modulations employing the same molecule type but with different labeling.[2] In these papers, the capacity of the multiple-access channel (MAC) is simply computed as the sum of the capacity of the channels between each transmitter and the receiver. In [26], the expected concentration of trapped molecules is computed. By approximating the number of delivered molecules as a normally distributed random variable, the maximum detection probability is calculated which the capacity is then computed. In [27], the channel randomness effect has been modeled by adding an additive Gaussian noise to the concentration of trapped molecules. Then, by using the Gaussian approximation, the capacity of each user channel is derived. In [28], the capacity of each user channel is computed by representing the diffusion channel as a binary test channel. In all these works, the average interference from the other transmitters is taken into account in calculating the binding probability. Unlike the previous works, here we examine the instantaneous effect of the multiple-access interference instead of its average value.

We first concentrate on a point-to-point memoryless molecular communication and evaluate its capacity and then propose new upper and lower bounds. Next, we consider three multiple-access scenarios and evaluate the capacity region and inner bounds for each scenario. Our main contributions are as follows.

Point-to-Point Communication: We investigate the trade-offs between two point-to-point bacterial communication scenarios via ligand-receptors with a fixed total number of molecules and receptors: (a) multi-type molecular communication with a single concentration level, and (b) single-type molecular communication with multiple concentration levels. At first glance, scenario (a) introduces new degrees of freedom and should reduce the ISI. However, since the number of molecules per type (the power per type) reduces when the number of types increases, we must asses the benefits of using different molecule types. To make a fair comparison between scenario (a) and (b), we adopt the model of [17] in this work. In addition, a Markov model for the interference between different molecule types near the receptor is presented and the capacity for this model is computed numerically.

Upper and Lower Bounds for the memoryless BIC Capacity: Using the Kullback-Leibler (KL) divergence bound in [16], we derive an upper bound on the capacity of the point-to-point memoryless BIC model under given average and peak constraints on the channel input (Theorem 1). Based on the numerical evidence, we believe that this upper bound works well in the low SNR regime. This upper bound results an upper performance limit for the case with ISI. A lower bound is derived on the point-to-point BIC capacity under average and peak constraints in the case of no environmental noise in Lemma 1.

Multiple-Access Communication: We investigate the trade-offs among three multiple-access bacterial communication scenarios for ligand-receptors with a fixed total number of receptors:

(a) Using the same molecule type with different labeling for different transmitters and a single receptor type at the receiver (DLSR).

(b) Using different molecule types for different transmitters and different receptor types at the receiver (DMDR).

[2]Mainly three kinds of labeling processes are used, which are radio, enzymatic, and fluorescent labeling [29].

(c) Using the same molecule type for the transmitters and a single receptor type at the receiver (SMSR).

Scenarios (a) and (c), both have a single type receptor and introduce a new degree of freedom. However, the benefit of using different types of molecules in scenario (b) should be examined. Scenario (a) has also the advantage that the transmitters use a self-identifying label and therefore seems to have better performance than scenarios (b) and (c). To compare the three scenarios, we compute their total capacities numerically. By assuming two transmitters in Section V-A, we derive some inner bounds on the capacity region of the three scenarios under average and peak constraints in the case of no environmental noise.

All logarithms are in base e in this paper. We also assume that the environment is unbounded. Throughout the paper, $H(p) = -p\log p - (1-p)\log(1-p)$ and $g(p) = \frac{H(p)}{1-p}$. This paper is organized as follows: in Section II, we present the system model for point-to-point communication scenarios, whose capacities are discussed in Section III. The interaction of molecules near the receptors is modeled in Section II-A. In Section III-A, a new upper bound on the capacity of the BIC is presented by considering peak and average constraints. Section III-B includes a lower bound on the capacity of the BIC by extending the Z-channel. In Section IV, three scenarios for multiple-access communications are presented, where their capacity regions and total capacities are discussed in Section V. The achievable rates for these scenarios are provided in Section V-A. Section VI includes the numerical results, and finally concluding remarks are given in Section VII.

II. Point-to-Point System Model

In this section, we describe two bacterial point-to-point communication scenarios with ligand-receptors.

Level Scenario (LS): Here, the transmitter encodes information at multiple concentration levels to create the codewords. At the transmitter and the receiver, there is only one colony with n bacteria where each bacteria has N receptors; i.e., nN receptors in total. All these n bacteria at the transmitter produce the same molecule type.

Type Scenario (TS): This scenario uses multiple molecule types at the transmitter and the receiver. We assume the same total number of n bacteria (as in LS) are available which are equally divided into m colonies at both the transmitter and receiver. As such, each colony has n/m bacteria. Moreover, each colony at the transmitter produces a different type of Acyl Homoserine Lactones (AHL) molecules. Furthermore, the colonies are synchronized at the transmitter. Similar to the LS scenario, each bacteria has N receptors. Therefore, there are nN/m receptors in total per each colony, i.e., per each molecule type. Each colony can detect its own molecule type, and as a result, produces different color Fluorescent Proteins (e.g., GFP, YFP, ...) which are used by the receiver to decode the received signal. In addition, we assume that all receptors of a colony are independent and sense a common molecule concentration.

Given the complexity of the capacity problem for the BIC with memory, we assume an ISI-free communication in both scenarios. That is, we assume that the symbol duration is appropriate and there is an enzyme in the environment, which substantially reduces those molecules that do not bind to the receptors in the current time slot, and hence their interference with the molecules released in next time slots is negligible. This supports our memoryless assumption. We further assume that no attenuation occurs in the channel. Therefore, the received concentration $A_{\rm r}$ is equal to the transmitted concentration $A_{\rm s}$. At the receiver with ligand-receptors, the probability of binding, at the steady state is given by [17],

$$p_{\rm b} = \frac{A_{\rm s}}{A_{\rm s} + \frac{\kappa}{\gamma}}, \tag{1}$$

where γ is the input gain and κ is the dissociation rate of trapped molecules in the cell receptors. Similar to the other works, e.g., [11], for simplicity we assume that at the beginning of each slot, all receptors are unbound. Some measurement data for the probability of binding, i.e., (1), is provided in [30]. If we consider an environmental noise with concentration $A_{\rm ne}$, due to the molecules of the same type from other sources, the probability of binding becomes $p_{\rm b} = \frac{A_{\rm s}+A_{\rm ne}}{A_{\rm s}+A_{\rm ne}+\frac{\kappa}{\gamma}}$.

In LS, we only have one molecule type and its binding probability is equal to

$$p_{\rm b}^{\rm LS} = \frac{X + A_{\rm ne}^{\rm LS}}{X + A_{\rm ne}^{\rm LS} + \frac{\kappa}{\gamma}}, \tag{2}$$

where X is the received concentration at the receiver and $A_{\rm ne}^{\rm LS}$ is the concentration of the environmental noise. We can view the LS scenario as a BIC as follows:

$$\begin{aligned} &P^{\rm LS}(Y = y|X = x) \\ &\quad = \binom{nN}{y} f_{p_{\rm b}}^{y}\left(x + A_{\rm ne}^{\rm LS}\right)\left(1 - f_{p_{\rm b}}\left(x + A_{\rm ne}^{\rm LS}\right)\right)^{nN-y}, \\ &\quad f_{p_{\rm b}} : [0,\infty] \to [0,1],\ y \in \{0,1,\ldots,nN\}. \end{aligned} \tag{3}$$

The function $f_{p_{\rm b}}(.)$ is the binding probability function. From (2), we have $f_{p_{\rm b}}(X + A_{\rm ne}) = \frac{X+A_{\rm ne}}{X+A_{\rm ne}+\frac{\kappa}{\gamma}}$. As such, the function $f_{p_{\rm b}}(.)$ is an increasing and concave function.

In TS, we have different molecule types. Here, we assume that the binding processes of different molecule types are independent and every molecule only binds to its own receptor type. We investigate a more general model in Section II-A by taking into account the interaction of different molecule types in TS. The probability of binding for the i-th molecule type is given by

$$p_{{\rm b},i}^{\rm TS} = \frac{X_i + A_{{\rm ne},i}^{\rm TS}}{X_i + A_{{\rm ne},i}^{\rm TS} + \frac{\kappa_i}{\gamma_i}}, \tag{4}$$

where X_i is the received concentration of the i-th molecule type and $A_{{\rm ne},i}^{\rm TS}$ is the concentration of the environmental noise for the i-th molecule type. For the sake of simplicity in the capacity analysis, we assume $A_{{\rm ne},i}^{\rm TS} = A_{\rm ne}^{\rm TS}$ and the same parameters γ and κ for all types of molecules and receptors.

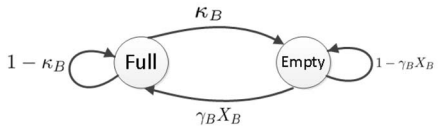

(a) With no blocking

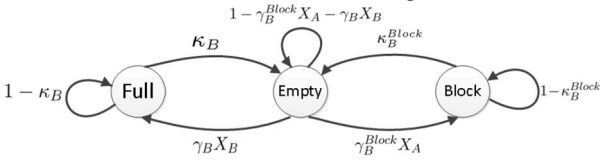

(b) With blocking

Fig. 1. Two Markov models for receptor type B.

This scenario can be viewed as m orthogonal BICs as follows:

$$P_i^{\mathrm{TS}}\left(Y_i = y_i \middle| X_i = x_i\right) = \binom{\frac{nN}{m}}{y_i} f_{p_{\mathrm{b}}}^{y_i}\left(x_i + A_{\mathrm{ne},i}^{\mathrm{TS}}\right)\left(1 - f_{p_{\mathrm{b}}}\left(x_i + A_{\mathrm{ne},i}^{\mathrm{TS}}\right)\right)^{\frac{nN}{m} - y_i}, \quad i = 1, \ldots, m, f_{p_{\mathrm{b}}} : [0, \infty] \to [0, 1], y_i \in \{0, 1, \ldots, \frac{nN}{m}\}. \tag{5}$$

A. Blocking of Receptors

In the TS scenario, we assume orthogonal parallel channels for different molecule types with no interference between them (i.e., no blocking of a receptor by molecules of another type). However, when there are different molecule types, they may interfere and collide with each other. In other words, one molecule type may block another molecule type from binding to its receptor counterpart. For example, consider $m = 2$ with two molecule types, A and B, and their corresponding receptors as R_A and R_B, respectively. The molecule type A, close to R_B, may prevent the molecule type B from binding to R_B (by just binding to R_B without activating it or by colliding with molecule type B). The blocking action is similar to antagonist function at biology [31]. Assume that X_A and X_B are the received concentrations of types A and B. The main reaction kinetics, for binding of the molecule type B to its receptor, is modeled as [5]

$$X_B + R_B \underset{\kappa_B}{\overset{\gamma_B}{\rightleftharpoons}} XR_B, \tag{6}$$

where $\gamma_B \geq 0$ is the association rate of the molecule type B with receptors of type B and $\kappa_B \geq 0$ is the dissociation rate of XR_B complex. Now, we characterize the blocking for the receptor type B, similar to the reaction kinetics formulas, by

$$X_A + R_B \xrightarrow{\gamma_B^{\mathrm{Block},A}} R_B^{\mathrm{Block},A}, X_A + R_B \xleftarrow{\kappa_B^{\mathrm{Block},A}} R_B^{\mathrm{Block},A} \tag{7}$$

where $\gamma_B^{\mathrm{Block},A} \geq 0$ is the blocking rate of R_B by molecule type A and $\kappa_B^{\mathrm{Block},A}$ is the unblocking rate of $R_B^{\mathrm{Block},A}$. If we do not take the blocking into account, then we have a reaction kinetics for each receptor type with its molecule type. As in [5], we define a Markov model for the no blocking case based on (6), as shown in Fig. 1a for $m = 2$. Likewise, according to (7), we propose a Markov model for the blocking case, as shown in Fig. 1b. We consider three states. The full state is when the receptor binds to its own type, the empty state is when the receptor is free, and the block state is when the receptor is blocked with a different molecule type. Solving the chain for the no blocking case, the steady state behavior of the system-reaction formula is obtained as (1). Solving the chain for the blocking case, we have the following probabilities of binding and blocking for the receptor type B:

$$p_{\mathrm{b}} = p_{\mathrm{Full}} = \frac{\frac{\gamma_B}{\kappa_B} X_B}{\frac{\gamma_B}{\kappa_B} X_B + \frac{\gamma_B^{\mathrm{Block},A}}{\kappa_B^{\mathrm{Block},A}} X_A + 1}, \quad p_{\mathrm{Block}} = \frac{\frac{\gamma_B^{\mathrm{Block},A}}{\kappa_B^{\mathrm{Block},A}} X_A}{\frac{\gamma_B}{\kappa_B} X_B + \frac{\gamma_B^{\mathrm{Block},A}}{\kappa_B^{\mathrm{Block},A}} X_A + 1}. \tag{8}$$

If we increase the concentration for one molecule type, the probability of binding for another type decreases as expected. This model can be extended for $m > 2$ via,

$$p_{\mathrm{b},i} = p_{\mathrm{Full},i} = \frac{\frac{\gamma_i}{\kappa_i} X_i}{\frac{\gamma_i}{\kappa_i} X_i + \sum_{j=1, j\neq i}^{m} \frac{\gamma_i^{\mathrm{Block},j}}{\kappa_i^{\mathrm{Block},j}} X_j + 1}, \quad p_{\mathrm{Block},i} = \frac{\sum_{j=1, j\neq i}^{m} \frac{\gamma_i^{\mathrm{Block},j}}{\kappa_i^{\mathrm{Block},j}} X_j}{\frac{\gamma_i}{\kappa_i} X_i + \sum_{j=1, j\neq i}^{m} \frac{\gamma_i^{\mathrm{Block},j}}{\kappa_i^{\mathrm{Block},j}} X_j + 1}, \tag{9}$$

where $p_{\mathrm{b},i}$ and $p_{\mathrm{Block},i}$ are the binding probability of the i-th type of receptor to the molecules of its own type and the blocking probability of the i-th type of receptor by the molecules of the other types, respectively. The blocking and unblocking rates for the i-th type of receptor by the molecules of the jth type are defined by $\gamma_i^{\mathrm{Block},j}$ and $\kappa_i^{\mathrm{Block},j}$, respectively. It is also possible to consider the environmental noise for the binding and blocking probabilities. Hence, the probability of binding for the i-th molecule type is given by

$$p_{\mathrm{b},i}^{\mathrm{TS,B}} = \frac{\frac{\gamma_i}{\kappa_i} X_{i,\mathrm{ne}}^{\mathrm{TS}}}{\frac{\gamma_i}{\kappa_i} X_{i,\mathrm{ne}}^{\mathrm{TS}} + \sum_{j=1, j\neq i}^{m} \frac{\gamma_i^{\mathrm{Block},j}}{\kappa_i^{\mathrm{Block},j}} X_{j,\mathrm{ne}}^{\mathrm{TS}} + 1}, \tag{10}$$

where $X_{i,\mathrm{ne}}^{\mathrm{TS}} = X_i + A_{\mathrm{ne},i}^{\mathrm{TS}}$. We can view the TS scenario with blocking as a multi-input multi-output BIC as follows:

$$P_i^{\mathrm{TS,B}}\left(Y_i = y_i \middle| X_1 = x_1, \ldots, X_m = x_m\right) = \binom{\frac{nN}{m}}{y_i} f_{p_{\mathrm{b},i}}^{y_i}\left(x_1, \ldots, x_m, A_{\mathrm{ne},i}^{\mathrm{TS}}\right) \times \left(1 - f_{p_{\mathrm{b},i}}\left(x_1, \ldots, x_m, A_{\mathrm{ne},i}^{\mathrm{TS}}\right)\right)^{\frac{nN}{m} - y_i}, \quad i = 1, \ldots, m, \tag{11}$$

where $f_{p_{\mathrm{b},i}}(X_1,\ldots,X_m,A^{\mathrm{TS}}_{\mathrm{ne},i}) = p^{\mathrm{TS},B}_{\mathrm{b},i}$ is the probability of binding when the blocking is considered.

III. Point-to-Point Capacity Analysis

We investigate the capacity for the two scenarios. In both scenarios, the output is discrete. Further, we take the environmental noise into account and assume average and peak constraints for the input concentration.

In LS, we have a single colony with input X and output Y. The peak and average constraints for the input concentration are $0 \le X \le A_s$ and $\mathbb{E}[X] \le \alpha_{\mathrm{s}} A_{\mathrm{s}}$, respectively, where $0 < \alpha_s < 1$. Then, we obtain the capacity for LS as

$$C_{\mathrm{LS}} = \max_{\substack{P(x):\\ 0\le X\le A_{\mathrm{s}},\ \mathbb{E}[X]\le \alpha_{\mathrm{s}}A_{\mathrm{s}}}} I(X;Y),\ \ Y\in\{0,1,\ldots,nN\}. \tag{12}$$

In TS, we use X_i to denote the input of the i-th colony to the channel and Y_i to denote the output of the i-th colony at the receiver. The peak and average constraints for the input concentration of the i-th colony are $0 \le X_i \le \frac{A_{\mathrm{s}}}{m}$ and $\mathbb{E}[X_i] \le \alpha_{\mathrm{s}}\frac{A_{\mathrm{s}}}{m}$, respectively, where $0 < \alpha_s < 1$. Hence, the capacity can be written as

$$C_{\mathrm{TS}} = \max_{\substack{P(x_1,x_2,\ldots,x_m):\\ 0\le X_i\le \frac{A_{\mathrm{s}}}{m},\ \mathbb{E}[X_i]\le \alpha_{\mathrm{s}}\frac{A_{\mathrm{s}}}{m}}} I(X_1,\ldots,X_m;Y_1,\ldots,Y_m),$$
$$Y_i \in \left\{0,1,\ldots,\frac{nN}{m}\right\}. \tag{13}$$

If we do not consider the blocking, the capacity could be obtained as follows:

$$C_{\mathrm{TS}} = m\times \max_{\substack{P(x_i):\\ 0\le X_i\le \frac{A_{\mathrm{s}}}{m},\ \mathbb{E}[X_i]\le \alpha_{\mathrm{s}}\frac{A_{\mathrm{s}}}{m}}} I(X_i;Y_i),$$
$$Y_i \in \left\{0,1,\ldots,\frac{nN}{m}\right\}. \tag{14}$$

For a fair comparison, we consider $A^{\mathrm{LS}}_{\mathrm{ne}} = A^{\mathrm{TS}}_{\mathrm{ne}} = A_{\mathrm{ne}}$. Since we have a BIC in LS and m parallel BICs in TS with no blocking, we consider a BIC for the two scenarios as follows:

$$P(Y=y|X=x) = \binom{N'}{y} f^y_{p_{\mathrm{b}}}(x+A_{\mathrm{ne}})\big(1-f_{p_{\mathrm{b}}}(x+A_{\mathrm{ne}})\big)^{N'-y},$$
$$f_{p_{\mathrm{b}}}:[0,\infty]\to[0,1],\ \ y\in\{0,1,\ldots,N'\}. \tag{15}$$

Since $P(y|x)$ is a Binomial distribution, we have $\sum_y yP(y|x) = N' f_{p_{\mathrm{b}}}(x)$. The peak and average constraints for the input of the BIC are $0 \le X \le A'_{\mathrm{s}}$ and $\mathbb{E}[X] \le \alpha_{\mathrm{s}}A'_{\mathrm{s}}$, respectively, where $0 < \alpha_s < 1$. Note that for LS and TS we have the following parameters:

- **LS:** $N' = nN$ and $A'_{\mathrm{s}} = A_{\mathrm{s}}$.
- **TS with no blocking:** $N' = \frac{nN}{m}$ and $A'_{\mathrm{s}} = \frac{A_{\mathrm{s}}}{m}$.

A. Capacity Upper Bound

There is no closed form for the BIC capacity. As such, for the first time, we propose an upper bound on the capacity of the BIC at the low SNR regime by considering average and peak constraints using the symmetrized KL divergence, referred as KL upper bound in [16]. We first explain the KL upper bound, $\mathcal{U}(P(y|x))$, briefly. Let $D_{\mathsf{sym}}(p\|q) = D(p\|q) + D(q\|p)$. Then,

$$\mathcal{U}(P(y|x)) = \max_{P(x)} D_{\mathsf{sym}}(P(x,y)\|P(x)P(y)) \ge \max_{P(x)} I(X;Y) = C(P(y|x)). \tag{16}$$

The KL upper bound is always an upper bound on the capacity. It is straightforward to show that $D_{\mathsf{sym}}(P(x,y)\|P(x)P(y)) = \mathbb{E}_{P(x,y)}\log P(Y|X) - \mathbb{E}_{P(x)P(y)}\log P(Y|X)$. Now, we state our upper bound in the following theorem. The proof of this theorem can be found in Appendix A.

Theorem 1: Consider a point-to-point BIC as in (15) and any input probability mass function (p.m.f) $P(x)$. Then, the symmetrized KL divergence upper bound has the following explicit formula:

$$I(X;Y) \le \mathcal{U}(P(x,y)) = N'\mathsf{Cov}\left(f_{p_{\mathrm{b}}}(X+A_{\mathrm{ne}}), \log\left(\frac{f_{p_{\mathrm{b}}}(X+A_{\mathrm{ne}})}{1-f_{p_{\mathrm{b}}}(X+A_{\mathrm{ne}})}\right)\right), \tag{17}$$

where $\mathsf{Cov}(X,Y) = \mathbb{E}[XY] - \mathbb{E}[X]\mathbb{E}[Y]$. Furthermore, imposing the average intensity constraint $\alpha_{\mathrm{s}}A'_{\mathrm{s}}$ and peak constraint A'_{s}, we get

$$\mathcal{U}_{\mathsf{Binomial}}(P(y|x)) := \max_{\substack{P(x):\\ 0\le X\le A'_{\mathrm{s}},\ \mathbb{E}[X]=\alpha_{\mathrm{s}}A'_{\mathrm{s}}}} \mathcal{U}(P(x,y)) = N'\begin{cases} \dfrac{f_{p_{\mathrm{b}}}(\alpha_{\mathrm{s}}A'_{\mathrm{s}}+A_{\mathrm{ne}})}{f_{p_{\mathrm{b}}}(A'_{\mathrm{s}}+A_{\mathrm{ne}})}\times F\times E & \text{if } (*),\\ \dfrac{f_{p_{\mathrm{b}}}(A'_{\mathrm{s}}+A_{\mathrm{ne}})}{4}\times E & \text{if } (**),\end{cases} \tag{18}$$

where $E = \log\left(\frac{f_{p_{\mathrm{b}}}(A'_{\mathrm{s}}+A_{\mathrm{ne}})(1-f_{p_{\mathrm{b}}}(A_{\mathrm{ne}}))}{f_{p_{\mathrm{b}}}(A_{\mathrm{ne}})(1-f_{p_{\mathrm{b}}}(A'_{\mathrm{s}}+A_{\mathrm{ne}}))}\right)$, $F = [f_{p_{\mathrm{b}}}(A'_s+A_{\mathrm{ne}}) - f_{p_{\mathrm{b}}}(\alpha_{\mathrm{s}}A'_{\mathrm{s}}+A_{\mathrm{ne}})]$, $(*) : f_{p_{\mathrm{b}}}(\alpha_{\mathrm{s}}A'_{\mathrm{s}}+A_{\mathrm{ne}}) < \frac{f_{p_{\mathrm{b}}}(A'_{\mathrm{s}}+A_{\mathrm{ne}})}{2}$, and $(**) : f_{p_{\mathrm{b}}}(\alpha_{\mathrm{s}}A'_{\mathrm{s}}+A_{\mathrm{ne}}) \ge \frac{f_{p_{\mathrm{b}}}(A'_{\mathrm{s}}+A_{\mathrm{ne}})}{2}$. Hence,

$$C = \max_{\substack{P(x):\\ 0\le X\le A'_{\mathrm{s}},\ \mathbb{E}[X]=\alpha_{\mathrm{s}}A'_{\mathrm{s}}}} I(X;Y) \le \mathcal{U}_{\mathsf{Binomial}}(P(y|x)). \tag{19}$$

We compute this KL upper bound numerically in Section VI. Based on the numerical evidence, this upper bound works well for all Binomial channels (such as MC channels) with low capacity.

B. Capacity Lower Bound

We obtain a lower bound on the capacity of the BIC when the environmental noise is negligible. We assume a binary input, while in the previous section, a continuous input was assumed. Under this assumption, the resulted capacity is a lower bound on the capacity of the BIC. We compute a closed form formula for the lower bound in the following lemma.

Lemma 1: Consider a point-to-point BIC as in (15) and any input p.m.f $P(x)$, in which $A_{\mathrm{ne}} = 0$, $x \in \{0, A'_{\mathrm{s}}\}$, and $\mathbb{E}[X] \le \alpha_{\mathrm{s}}A'_{\mathrm{s}}$, where $0 < \alpha_s < 1$. The capacity of this channel is obtained as

$$C = \begin{cases} G(p_c), & \alpha_{\mathrm{s}} \ge \dfrac{1}{1-p_c+e^{\frac{-p_c\log p_c}{1-p_c}}},\\ f_I(\alpha_{\mathrm{s}},p_c), & 0<\alpha_{\mathrm{s}} < \dfrac{1}{1-p_c+e^{\frac{-p_c\log p_c}{1-p_c}}},\end{cases} \tag{20}$$

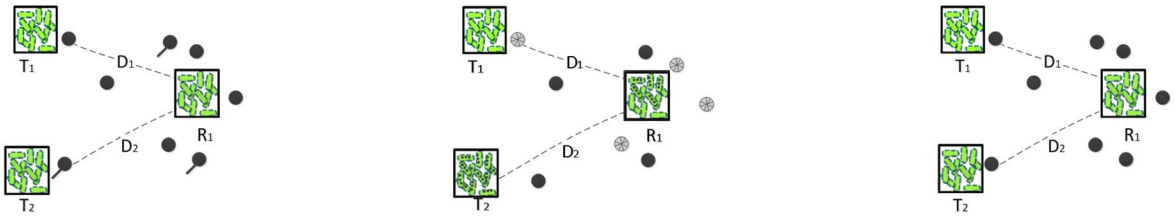

(a) DLSR scenario (b) DMDR scenario (c) SMSR scenario

Fig. 2. Three schemes of multiple-access in molecular communication systems.

where $G(p) = H(\frac{1}{1+e^{g(p)}}) - \frac{g(p)}{1+e^{g(p)}}$, $p_c = (\frac{\frac{\kappa}{\gamma}}{A'_s+\frac{\kappa}{\gamma}})^{N'}$, and $f_I(\alpha, p) = -\alpha(1-p)\log\alpha + \alpha p \log p - (1-\alpha+\alpha p)\log(1-\alpha+\alpha p)$.

Proof: The proof is provided in Appendix B. ■

If we consider $N' = 1$, then the channel would reduce to a Z-channel.

IV. Multiple-Access System Model

We describe three bacterial multiple-access communication scenarios with ligand-receptors based on molecule and receptor types various. **DLSR Scenario:** As shown in Fig. 2a, the transmitters send the same molecule type (AHL) with different labeling and the receiver employs one type of bacteria (receptor). At the receiver, there is only one colony with n bacteria where each bacteria has N receptors; i.e., nN receptors in total.

DMDR Scenario: As shown in Fig. 2b, each transmitter uses a different type of bacteria and so a different molecule type (AHL) and the receiver employs different types of bacteria (receptors). At the receiver, there are m different colonies with n/m bacteria where each bacteria type has N receptors; i.e., nN/m receptors in total for the i-th molecule type.

SMSR Scenario: As shown in Fig. 2c, the transmitters send the same molecule type (AHL) and the receiver employs one type of bacteria (receptor). At the receiver, there is only one colony with n bacteria, where each bacteria has N receptors; i.e., nN receptors in total.

In all scenarios, we assume that there is no ISI and no attenuation in the channel. Further, we assume that X_i is the received concentration from the i-th transmitter.

In the DLSR scenario, since different labeling are used [26]–[28], it is possible to distinguish between the molecules emitted from different transmitters. For example, consider $m = 2$ with two different labelings of a molecule, denoted by L_1 and L_2. Assume that X^{L_1} and X^{L_2} are the received concentrations of the labelings L_1 and L_2, respectively. The main reaction kinetics, for binding of the molecules with different labelings to the receptors, are modeled as

$$X^{L_1} + R \underset{\kappa}{\overset{\gamma}{\rightleftharpoons}} XR^{L_1}, \; X^{L_2} + R \underset{\kappa}{\overset{\gamma}{\rightleftharpoons}} XR^{L_2}, \tag{21}$$

where we consider the same association and dissociation rates for the two different labelings. Similar to the blocking case, we propose a Markov model for the labeling scenario, as shown in Fig. 3 for $m = 2$. The steady state behaviour of the system-reaction formula is obtained as

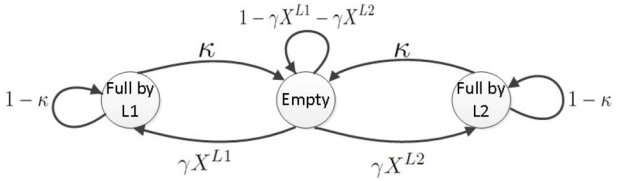

Fig. 3. Markov model for labeling.

$$p_{b,1} = \frac{X^{L_1}}{X^{L_1} + X^{L_2} + \frac{\kappa}{\gamma}}, \; p_{b,2} = \frac{X^{L_2}}{X^{L_1} + X^{L_2} + \frac{\kappa}{\gamma}}, \tag{22}$$

where $p_{b,1}$ and $p_{b,2}$ are the probabilities of being full by L_1 and L_2 for each receptor, respectively. This model can be extended for $m > 2$ via,

$$p_{b,i} = \frac{X^{L_i}}{\sum_{j=1}^{m} X^{L_j} + \frac{\kappa}{\gamma}}, \tag{23}$$

where $p_{b,i}$ is the binding probability of the receptors to the molecules with the i-th label type. It is also possible to consider the environmental noise for the binding probabilities:

$$p_{b,i}^{DLSR} = \frac{X_i + A_{ne,i}^{DLSR}}{\sum_{j=1}^{m}(X_j + A_{ne,j}^{DLSR}) + \frac{\kappa}{\gamma}}, \tag{24}$$

where $A_{ne_i}^{DLSR}$ is the concentration of the environmental noise for the molecules with the i-th label type. For simplicity, we assume $A_{ne,i}^{DLSR} = A_{ne}^{DLSR}$. Let the output Y_i be the number of receptors bound to the molecules with the i-th label type. The outputs, $(y_1, \ldots, y_m)$, along with the unbound state have multinomial distribution with parameters $p_{b,1}^{DLSR}, \ldots, p_{b,m}^{DLSR}$, $1 - \sum_{i=1}^{m} p_{b,i}^{DLSR}$:

$$\begin{aligned} &P^{DLSR}(y_1, \ldots, y_m | x_1, \ldots, x_m) \\ &= \binom{nN}{y_1} \cdots \binom{nN - \sum_{i=1}^{m-1} y_i}{y_m} \left(p_{b,1}^{DLSR}\right)^{y_1} \cdots \left(p_{b,m}^{DLSR}\right)^{y_m} \\ &\quad \times \left(1 - \sum_{i=1}^{m} p_{b,i}^{DLSR}\right)^{nN - \sum_{i=1}^{m} y_i}. \end{aligned} \tag{25}$$

In the DMDR scenario, we have different molecule types for the transmitters. Without blocking, the binding probability

TABLE I
VARIABLES OF THE MULTIPLE-ACCESS SCENARIOS

Variable	Definition
$p_{\mathrm{b},i}^{\mathrm{DLSR}}$, $p_{\mathrm{b},i}^{\mathrm{DMDR}}$, $p_{\mathrm{b}}^{\mathrm{SMSR}}$, $p_{\mathrm{b},i}^{\mathrm{DMDR,B}}$	$\frac{X_i+A_{\mathrm{ne},i}^{\mathrm{DLSR}}}{\sum_{j=1}^{m}(X_j+A_{\mathrm{ne},j}^{\mathrm{DLSR}})+\frac{\kappa}{\gamma}}$, $\frac{X_i+A_{\mathrm{ne},i}^{\mathrm{DMDR}}}{X_i+A_{\mathrm{ne},i}^{\mathrm{DMDR}}+\frac{\kappa_i}{\gamma_i}}$, $\frac{\sum_{i=1}^{m}X_i+A_{\mathrm{ne}}^{\mathrm{SMSR}}}{\sum_{i=1}^{m}X_i+A_{\mathrm{ne}}^{\mathrm{SMSR}}+\frac{\kappa}{\gamma}}$, $\frac{\frac{\gamma_i}{\kappa_i}X_{i,\mathrm{ne}}^{\mathrm{DMDR}}}{\frac{\gamma_i}{\kappa_i}X_{i,\mathrm{ne}}^{\mathrm{DMDR}}+\sum_{j=1,j\neq i}^{m}\frac{\gamma_i^{\mathrm{Block},j}}{\kappa_i^{\mathrm{Block},j}}X_{j,\mathrm{ne}}^{\mathrm{DMDR}}+1}$
$P^{\mathrm{DLSR}}(y_1,...,y_m\|x_1,...,x_m)$	$\binom{nN}{y_1}...\binom{nN-\sum_{i=1}^{m-1}y_i}{y_m}\left(p_{\mathrm{b},1}^{\mathrm{DLSR}}\right)^{y_1}...\left(p_{\mathrm{b},m}^{\mathrm{DLSR}}\right)^{y_m}\left(1-\sum_{i=1}^{m}p_{\mathrm{b},i}^{\mathrm{DLSR}}\right)^{nN-\sum_{i=1}^{m}y_i}$
$P^{\mathrm{DMDR}}(y_1,...,y_m\|x_1,...,x_m)$	$\prod_{i=1}^{m}\binom{\frac{nN}{m}}{y_i}\left(p_{\mathrm{b},i}^{\mathrm{DMDR}}\right)^{y_i}\left(1-p_{\mathrm{b},i}^{\mathrm{DMDR}}\right)^{\frac{nN}{m}-y_i}$
$P^{\mathrm{DMDR,B}}(y_1,...,y_m\|x_1,...,x_m)$	$\prod_{i=1}^{m}\binom{\frac{nN}{m}}{y_i}\left(p_{\mathrm{b},i}^{\mathrm{DMDR,B}}\right)^{y_i}\left(1-p_{\mathrm{b},i}^{\mathrm{DMDR,B}}\right)^{\frac{nN}{m}-y_i}$
$P^{\mathrm{SMSR}}(y\|x_1,...,x_m)$	$\binom{nN}{y}\left(p_{\mathrm{b}}^{\mathrm{SMSR}}\right)^{y}\left(1-p_{\mathrm{b}}^{\mathrm{SMSR}}\right)^{nN-y}$

for the i-th molecule type is obtained as

$$p_{\mathrm{b},i}^{\mathrm{DMDR}}=\frac{X_i+A_{\mathrm{ne},i}^{\mathrm{DMDR}}}{X_i+A_{\mathrm{ne},i}^{\mathrm{DMDR}}+\frac{\kappa_i}{\gamma_i}},\tag{26}$$

where $A_{\mathrm{ne},i}^{\mathrm{DMDR}}$ is the concentration of the environmental noise for the i-th type molecules. For simplicity, we assume $A_{\mathrm{ne},i}^{\mathrm{DMDR}}=A_{\mathrm{ne}}^{\mathrm{DMDR}}$. Let the output Y_i be the number of receptors bound to the i-th type molecules. Then, $Y_i\sim\mathrm{Binomial}\left(\frac{nN}{m},p_{\mathrm{b},i}^{\mathrm{DMDR}}\right)$ and

$$\begin{aligned}&P^{\mathrm{DMDR}}(y_1,\ldots,y_m|x_1,\ldots,x_m)\\&\quad=\prod_{i=1}^{m}P(Y_i=y_i|X_i=x_i)\\&\quad=\prod_{i=1}^{m}\binom{\frac{nN}{m}}{y_i}\left(p_{\mathrm{b},i}^{\mathrm{DMDR}}\right)^{y_i}\left(1-p_{\mathrm{b},i}^{\mathrm{DMDR}}\right)^{\frac{nN}{m}-y_i}.\end{aligned}\tag{27}$$

However, by considering the blocking, taking the same steps as deriving (9), we have the following binding probability for the i-th molecule type:

$$p_{\mathrm{b},i}^{\mathrm{DMDR,B}}=\frac{\frac{\gamma_i}{\kappa_i}X_{i,\mathrm{ne}}^{\mathrm{DMDR}}}{\frac{\gamma_i}{\kappa_i}X_{i,\mathrm{ne}}^{\mathrm{DMDR}}+\sum_{j=1,j\neq i}^{m}\frac{\gamma_i^{\mathrm{Block},j}}{\kappa_i^{\mathrm{Block},j}}X_{j,\mathrm{ne}}^{\mathrm{DMDR}}+1},\tag{28}$$

where $X_{i,\mathrm{ne}}^{\mathrm{DMDR}}=X_i+A_{\mathrm{ne},i}^{\mathrm{DMDR}}$. Here, we have $Y_i\sim\mathrm{Binomial}(\frac{nN}{m},p_{\mathrm{b},i}^{\mathrm{DMDR,B}})$ and

$$\begin{aligned}&P^{\mathrm{DMDR,B}}(y_1,\ldots,y_m|x_1,\ldots,x_m)\\&\quad=\prod_{i=1}^{m}P(Y_i=y_i|X_1=x_1,\ldots,X_m=x_m)\\&\quad=\prod_{i=1}^{m}\binom{\frac{nN}{m}}{y_i}\left(p_{\mathrm{b},i}^{\mathrm{DMDR,B}}\right)^{y_i}\left(1-p_{\mathrm{b},i}^{\mathrm{DMDR,B}}\right)^{\frac{nN}{m}-y_i}.\end{aligned}\tag{29}$$

In the SMSR scenario, we have one molecule type for the transmitters. The receiver senses the sum of the concentrations X_i. Hence, the probability of binding is equal to

$$p_{\mathrm{b}}^{\mathrm{SMSR}}=\frac{\sum_{i=1}^{m}X_i+A_{\mathrm{ne}}^{\mathrm{SMSR}}}{\sum_{i=1}^{m}X_i+A_{\mathrm{ne}}^{\mathrm{SMSR}}+\frac{\kappa}{\gamma}},\tag{30}$$

where $A_{\mathrm{ne}}^{\mathrm{SMSR}}$ is the environmental noise. Let the output Y be the number of bound receptors. Then, $Y\sim\mathrm{Binomial}\left(nN,p_{\mathrm{b}}^{\mathrm{SMSR}}\right)$ and

$$P^{\mathrm{SMSR}}(y|x_1,\ldots,x_m)=\binom{nN}{y}\left(p_{\mathrm{b}}^{\mathrm{SMSR}}\right)^{y}\left(1-p_{\mathrm{b}}^{\mathrm{SMSR}}\right)^{nN-y}.\tag{31}$$

Table I summarizes the variables defined in this section.

V. MULTIPLE-ACCESS CAPACITY REGION ANALYSIS

In this section, we investigate the capacity region of the MAC for the three scenarios. In all scenarios, the output is discrete. Further, we consider peak and average constraints for the input concentration of the i-th transmitter as $0\leq X_i\leq A_{\mathrm{s},i}$ and $\mathbb{E}[X_i]\leq\alpha_{\mathrm{s},i}A_{\mathrm{s},i}$, where $0<\alpha_{\mathrm{s},i}<1$. We also take the environmental noise into account.

The DMDR scenario with no blocking can be viewed as m orthogonal point-to-point channels and the capacity of each channel can be computed according to Section III. So here, we consider the blocking. Since we have one receiver with m outputs in the DLSR and DMDR scenarios, we may view these scenarios as SIMO (single transmit antenna and multiple receive antennas) MACs and compute the capacity region as the convex hull of rate tuples $(R_1,\ldots,R_m)$ such that [32], $\sum_{i\in I}R_i\leq I(X(I);(Y_1,..,Y_m)|X(I^c))$, $\forall I\subseteq\{1,\ldots,m\}$, for some p.m.f $\prod_{i=1}^{k}P(x_i)$ that satisfies $0\leq X_i\leq A_{\mathrm{s},i}$, $\mathbb{E}[X_i]\leq\alpha_{\mathrm{s},i}A_{\mathrm{s},i}$, $i=1,\ldots,m$. The total capacity in these scenarios can be computed as follows:

$$C_{\mathrm{total}}^{\mathrm{DLSR,DMDR}}=\max_{\substack{P(x_1,x_2,\ldots,x_m)\ :\\0\leq X_i\leq A_{\mathrm{s},i},\\\mathbb{E}[X_i]\leq\alpha_{\mathrm{s},i}A_{\mathrm{s},i},\\i=1,\ldots,m}}I(X_1,\ldots,X_m;Y_1,\ldots,Y_m).\tag{32}$$

The SMSR scenario can be viewed as a SISO (single transmit antenna and single receive antenna) MAC. The capacity region of this channel is the convex hull of rate tuples $(R_1,\ldots,R_m)$ such that [32], $\sum_{i\in I}R_i\leq I(X(I);Y|X(I^c))\ \forall I\subseteq\{1,\ldots,m\}$, for some p.m.f $\prod_{i=1}^{k}P(x_i)$ that satisfies $0\leq X_i\leq A_{\mathrm{s},i}$, $\mathbb{E}[X_i]\leq\alpha_{\mathrm{s},i}A_{\mathrm{s},i}$, $i=1,\ldots,m$. The total capacity in this scenario can be computed as follows:

$$C_{\mathrm{total}}^{\mathrm{SMSR}}=\max_{\substack{P(x_1,x_2,\ldots,x_m)\ :\\0\leq X_i\leq A_{\mathrm{s},i},\ \mathbb{E}[X_i]\leq\alpha_{\mathrm{s},i}A_{\mathrm{s},i},\\i=1,\ldots,m}}I(X_1,\ldots,X_m;Y).\tag{33}$$

There is no algorithm to compute the capacity region of the MAC numerically [33]. Instead, the total capacities of the three

scenarios are computed numerically in Sention VI. We remark that the total capacity in the MAC is active and therefore it is sensible to compute it. For a fair comparison, we consider $A_{\rm ne}^{\rm DLSR} = A_{\rm ne}^{\rm DMDR} = A_{\rm ne}^{\rm SMSR} = A_{\rm ne}$.

A. Capacity Region Inner Bounds

We consider two transmitters and obtain inner bounds on the capacity region of the multiple-access communication in the three scenarios when the environmental noise is negligible. We assume a binary input to derive an inner bound, which is computed numerically in Section VI.

DLSR, DMDR: We may view the DLSR and DMDR scenarios as interference channels with full receiver cooperation. The capacity region of the interference channel is an inner bound on the capacity region of this channel. The time-division (TD) inner bound for an interference channel consists of all rate pairs (R_1, R_2) such that

$$R_1 < k\ C_1, R_2 < (1-k)\ C_2, \tag{34}$$

for some $k \in [0,1]$, where $C_1 = \max_{x_2,\ P(x_1)} I(X_1; Y_1|X_2 = x_2)$ and $C_2 = \max_{x_1,\ P(x_2)} I(X_2; Y_2|X_1 = x_1)$ are the maximum achievable individual rates [32]. This inner bound is computed in Lemma 2 for the DLSR and DMDR scenarios with binary inputs and considering peak and average constraints for the input concentration. It is shown in this lemma, whose proof is provided in Appendix C, that the maximum achievable individual rate for each transmitter in the two scenarios occurs when the concentration of the other transmitter is zero and therefore the closed form formulas for the maximum achievable individual rates are obtained. The interference-as-noise (IAN) inner bound for an interference channel consists of all rate pairs (R_1, R_2) such that [32], $R_1 < I(X_1; Y_1)$, $R_2 < I(X_2; Y_2)$, for some p.m.f $P(x_1)P(x_2)$. This inner bound is computed in Lemma 3 for the two scenarios with binary inputs and considering peak and average input constraints. The proof of this lemma is provided in Appendix D.

Lemma 2: Consider interference channels with two sender-receiver pairs and $P^{\rm DLSR}(y_1, y_2|x_1, x_2)$, $P^{\rm DMDR,B}(y_1, y_2|x_1, x_2)$, and any input p.m.f $P(x_1)P(x_2)$, in which $A_{\rm ne}^{\rm DLSR} = A_{\rm ne}^{\rm DMDR} = 0$, $x_1 \in \{0, A_{\rm s,1}\}$, $x_2 \in \{0, A_{\rm s,2}\}$, $\mathbb{E}[X_1] \le \alpha_{\rm s,1}A_{\rm s,1}$, and $\mathbb{E}[X_2] \le \alpha_{\rm s,2}A_{\rm s,2}$. The TD inner bound on the capacity region of these channels is obtained as

$$R_1 < kC_1,\ R_2 < (1-k)C_2,$$
$$C_i = \begin{cases} G\big(p_{c_{i0}}\big), & \alpha_{{\rm s},i} \ge \dfrac{1}{1-p_{c_{i0}}+e^{\frac{-p_{c_{i0}}\log p_{c_{i0}}}{1-p_{c_{i0}}}}}, \\ f_I\big(\alpha_{{\rm s},i}, p_{c_{i0}}\big), & 0 < \alpha_{{\rm s},i} < \dfrac{1}{1-p_{c_{i0}}+e^{\frac{-p_{c_{i0}}\log p_{c_{i0}}}{1-p_{c_{i0}}}}}, \end{cases} \tag{35}$$

for $i = 1, 2$ and some $k \in [0, 1]$, where $G(p) = H(\frac{1}{1+e^{g(p)}}) - \frac{g(p)}{1+e^{g(p)}}$ and $f_I(\alpha, p) = -\alpha(1-p)\log\alpha + \alpha p \log p - (1-\alpha+\alpha p)\log(1-\alpha+\alpha p)$. For the DLSR scenario, $p_{c_{i0}} = (\frac{\frac{\kappa}{\gamma}}{A_{{\rm s},i}+\frac{\kappa}{\gamma}})^{nN}$, $i = 1, 2$, and for the DMDR scenario with blocking, $p_{c_{i0}} = (\frac{\frac{\kappa_i}{\gamma_i}}{A_{{\rm s},i}+\frac{\kappa_i}{\gamma_i}})^{\frac{nN}{2}}$, $i = 1, 2$.

Lemma 3: Consider interference channels with two sender-receiver pairs and $P^{\rm DLSR}(y_1, y_2|x_1, x_2)$, $P^{\rm DMDR,B}(y_1, y_2|x_1, x_2)$, and any input p.m.f $P(x_1)P(x_2)$, in which $A_{\rm ne}^{\rm DLSR} = A_{\rm ne}^{\rm DMDR} = 0$, $x_1 \in \{0, A_{\rm s,1}\}$, $x_2 \in \{0, A_{\rm s,2}\}$, $\mathbb{E}[X_1] \le \alpha_{\rm s,1}A_{\rm s,1}$, and $\mathbb{E}[X_2] \le \alpha_{\rm s,2}A_{\rm s,2}$. The IAN inner bound on the capacity region of these channels is obtained as

$$\begin{aligned} R_i < &-\log\alpha_i + \alpha_i J\big(\alpha_{ji}, p_{c_{i0}}, p_{c_{i1}}\big)\log J\big(\alpha_{ji}, p_{c_{i0}}, p_{c_{i1}}\big) \\ &- \alpha_i\left(\frac{1-\alpha_i}{\alpha_i} + J\big(\alpha_{ji}, p_{c_{i0}}, p_{c_{i1}}\big)\right) \\ &\times\ \log\left(\frac{1-\alpha_i}{\alpha_i} + J\big(\alpha_{ji}, p_{c_{i0}}, p_{c_{i1}}\big)\right), \end{aligned} \tag{36}$$

for $i = 1, 2$ and some $\alpha_1 \in [0, \alpha_{\rm s,1}]$, $\alpha_2 \in [0, \alpha_{\rm s,2}]$, where $j_1 = 2$ and $j_2 = 1$ and $J(\alpha, p_1, p_2) = (1-\alpha)p_1 + \alpha p_2$. For the DLSR scenario, $p_{c_{i0}} = (\frac{\frac{\kappa}{\gamma}}{A_{{\rm s},i}+\frac{\kappa}{\gamma}})^{nN}$, $p_{c_{i1}} = (\frac{A_{{\rm s},j_i}+\frac{\kappa}{\gamma}}{A_{{\rm s},i}+A_{{\rm s},j_i}+\frac{\kappa}{\gamma}})^{nN}$, $i = 1, 2$ and for the DMDR scenario with blocking, $p_{c_{i0}} = (\frac{\frac{\kappa_i}{\gamma_i}}{A_{{\rm s},i}+\frac{\kappa_i}{\gamma_i}})^{\frac{nN}{2}}$, $p_{c_{i1}} = (\frac{\frac{\gamma_i}{\kappa_i}^{\rm Block,j_i}A_{{\rm s},j_i}+1}{\frac{\gamma_i}{\kappa_i}A_{{\rm s},i}+\frac{\gamma_i}{\kappa_i}^{\rm Block,j_i}A_{{\rm s},j_i}+1})^{\frac{nN}{2}}$, $i = 1, 2$, where $j_1 = 2$ and $j_2 = 1$.

For $A_{\rm s,1} = A_{\rm s,2} = A_{\rm s}$, we have $p_{c_{10}} = p_{c_{20}}$ and $p_{c_{11}} = p_{c_{21}}$. Assume $\alpha_{\rm s,1} = \alpha_{\rm s,2} = \alpha_{\rm s}$. The points where $R_1 = R_2$ are obtained when $\alpha_1 = \alpha_2$ and are computed as follows:

$$\begin{aligned} R_1 = R_2 = k\Bigg[&-\log\alpha' + \alpha' J\big(\alpha', p_{c_{10}}, p_{c_{11}}\big) \\ &\times\ \log J\big(\alpha', p_{c_{10}}, p_{c_{11}}\big) - \alpha'\left(\frac{1-\alpha'}{\alpha'} + J\big(\alpha', p_{c_{10}}, p_{c_{11}}\big)\right) \\ &\times\ \log\left(\frac{1-\alpha'}{\alpha'} + J\big(\alpha', p_{c_{10}}, p_{c_{11}}\big)\right)\Bigg], \end{aligned} \tag{37}$$

for some $k \in [0, 1]$, where $\alpha' = \min\{\alpha, \alpha_{\rm s}\}$ and α is the solution of the following equation:

$$\begin{aligned} &\big((1-2\alpha)p_{c_{10}} + 2\alpha p_{c_{11}}\big)\log J\big(\alpha, p_{c_{10}}, p_{c_{11}}\big) \\ &\quad - \big((1-2\alpha)p_{c_{10}} + 2\alpha p_{c_{11}} - 1\big) \\ &\quad \times\ \log\left(\frac{1-\alpha}{\alpha} + J\big(\alpha, p_{c_{10}}, p_{c_{11}}\big)\right) = 0. \end{aligned} \tag{38}$$

SMSR: As mentioned before, we may view the SMSR scenario as an SISO MAC. According to [32], the maximum achievable individual rates for a MAC are $C_1 = \max_{x_2,\ P(x_1)} I(X_1; Y|X_2 = x_2)$ and $C_2 = \max_{x_1,\ P(x_2)} I(X_2; Y|X_1 = x_1)$. Using these rates, the TD inner bound can be obtained as (34). This inner bound is computed in Lemma 4 for the SMSR scenario with binary input and considering peak and average input constraints. The proof of this lemma is provided in Appendix E.

Lemma 4: Consider a MAC with two transmitters and $P^{\rm SMSR}(y|x_1, x_2)$ and any input p.m.f $P(x_1)P(x_2)$, in which $A_{\rm ne}^{\rm SMSR} = 0$, $x_1 \in \{0, A_{\rm s,1}\}$, $x_2 \in \{0, A_{\rm s,2}\}$, $\mathbb{E}[X_1] \le \alpha_{\rm s,1}A_{\rm s,1}$,

and $\mathbb{E}[X_2] \leq \alpha_{\mathrm{s},2} A_{\mathrm{s},2}$. The TD inner bound on the capacity region of this channel is obtained as

$$R_1 < k \max\{c_{10}, c_{11}\}, \;\; R_2 < (1-k)\max\{c_{20}, c_{21}\},$$

$$c_{i0} = \begin{cases} G\big(p_{c_{i0}}\big), & \alpha_{\mathrm{s},i} \geq \dfrac{1}{1-p_{c_{i0}}+e^{\frac{-p_{c_{i0}}\log p_{c_{i0}}}{1-p_{c_{i0}}}}}, \\ f_I\big(\alpha_{\mathrm{s},i}, p_{c_{i0}}\big), & 0 < \alpha_{\mathrm{s},i} < \dfrac{1}{1-p_{c_{i0}}+e^{\frac{-p_{c_{i0}}\log p_{c_{i0}}}{1-p_{c_{i0}}}}}, \end{cases}$$

$$c_{i1} = -\sum_{y=0}^{nN}\Bigg[\big(1-\alpha_i'\big)P^i_{y|0,A_{\mathrm{s},j_i}} \times \log\left(\big(1-\alpha_i'\big)+\alpha_i'\frac{P^i_{y|A_{\mathrm{s},i},A_{\mathrm{s},j_i}}}{P^i_{y|0,A_{\mathrm{s},j_i}}}\right) + \alpha_i' P^i_{y|A_{\mathrm{s},i},A_{\mathrm{s},j_i}} \log\left(\big(1-\alpha_i'\big)\frac{P^i_{y|0,A_{\mathrm{s},j_i}}}{P^i_{y|A_{\mathrm{s},i},A_{\mathrm{s},j_i}}}+\alpha_i'\right)\Bigg], \tag{39}$$

for $i = 1, 2$ and some $k \in [0, 1]$, where $j_1 = 2$, $j_2 = 1$, $G(p) = H(\frac{1}{1+e^{g(p)}}) - \frac{g(p)}{1+e^{g(p_{c_{i0}})}}$, $f_I(\alpha, p) = -\alpha(1-p)\log\alpha + \alpha p \log p - (1-\alpha+\alpha p)\log(1-\alpha+\alpha p)$, $P^i_{y|x_1,x_2} = P(Y = y|X_i = x_1, X_{j_i} = x_2)$, $p_{c_{i0}} = (\frac{\frac{\kappa}{\gamma}}{A_{\mathrm{s},i}+\frac{\kappa}{\gamma}})^{nN}$, $i = 1, 2$, and $\alpha_i' = \min\{\alpha_i, \alpha_{\mathrm{s},i}\}$, where α_i, $i = 1, 2$ is the solution of the following equation:

$$\sum_{y=0}^{nN}\Bigg[P^i_{y|0,A_{\mathrm{s},j_i}} \log\left((1-\alpha_i)+\alpha_i\frac{P^i_{y|A_{\mathrm{s},i},A_{\mathrm{s},j_i}}}{P^i_{y|0,A_{\mathrm{s},j_i}}}\right) - P^i_{y|A_{\mathrm{s},i},A_{\mathrm{s},j_i}} \log\left((1-\alpha_i)\frac{P^i_{y|0,A_{\mathrm{s},j_i}}}{P^i_{y|A_{\mathrm{s},i},A_{\mathrm{s},j_i}}}+\alpha_i\right)\Bigg] = 0, \tag{40}$$

where $j_1 = 2$ and $j_2 = 1$.

VI. Numerical Results

In this section, we first consider a point-to-point communication, and evaluate the rates for the TS and LS scenarios as well as the lower and KL upper bounds. Then, we evaluate the total capacity and achievable rates for the three scenarios of the multiple-access communications. We set $\gamma = \gamma_1 = \cdots = \gamma_m = 0.0004$ (nM min)$^{-1}$ and $\kappa = \kappa_1 = \cdots = \kappa_m = 0.1$ min^{-1}, consistent with the parameters in [17], where the unit of the concentration of molecules is nano-Moles per litre (nM). We consider two blocking cases:

Low Blocking: $\gamma_1^{\mathrm{Block},2} = \gamma_2^{\mathrm{Block},1} = 0.0003$ (nM min)$^{-1}$, $\kappa_1^{\mathrm{Block},2} = \kappa_2^{\mathrm{Block},1} = 0.15$ min^{-1}.

High Blocking: $\gamma_1^{\mathrm{Block},2} = \gamma_2^{\mathrm{Block},1} = 0.0005$ (nM min)$^{-1}$, $\kappa_1^{\mathrm{Block},2} = \kappa_2^{\mathrm{Block},1} = 0.01$ min^{-1}.

A. Point-to-Point Capacity for LS and TS and Effect of Blocking

We evaluate the rates of the TS scenario given in (14) and the LS scenario given in (12), using the Blahut-Arimoto (BA) algorithm [34]. We assume $N = 10$ and $n = 16$. Note that we consider small values of N and n to reduce the time complexity of the BA algorithm, although these values can be very large in practice.

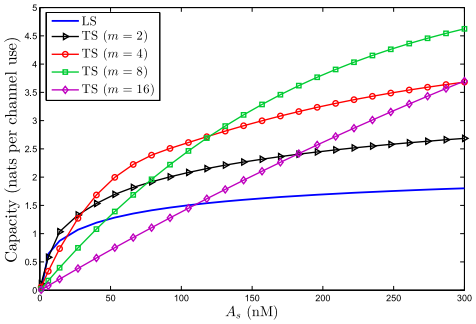

(a) $A_{\mathrm{ne}}^{\mathrm{LS}} = A_{\mathrm{ne}}^{\mathrm{TS}} = 0$

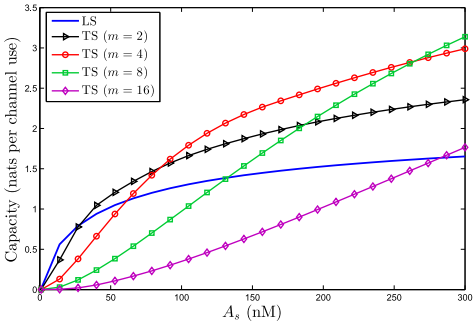

(b) $A_{\mathrm{ne}}^{\mathrm{LS}} = A_{\mathrm{ne}}^{\mathrm{TS}} = 5$

Fig. 4. Capacity of TS with no blocking and LS for $\alpha_{\mathrm{s}} = \frac{1}{2}$.

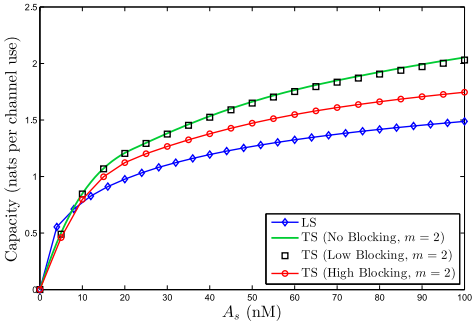

Fig. 5. Capacity of TS with and without blocking and LS for $\alpha_{\mathrm{s}} = \frac{1}{2}$ and $A_{\mathrm{ne}} = 0$.

Fig. 4a shows the capacity of TS with no blocking and LS, for $m = 2, 4, 8, 16$ when $A_{\mathrm{ne}}^{\mathrm{LS}} = A_{\mathrm{ne}}^{\mathrm{TS}} = 0$. It is seen that increasing the number of molecule types, m, improves the performance (for fixed A_{s}), which is expected due to the parallel transmission of the molecules. However, if we continue to increase m, and accordingly decrease the number of bacteria in each colony to n/m, the performance degrades. The reason is that decreasing the concentration level of TS in (4) decreases the binding probability. Hence, there exists an optimal m. For example, for $A_{\mathrm{s}} = 80$, this optimal value lies between $m = 4$ and $m = 8$. This implies that for $A_{\mathrm{s}} = 80$ and $m = 2, 4$, the capacity of TS is higher than LS, whereas for $m = 8, 16$, the capacity of TS is lower than LS. Similar conclusions can be made from Fig. 4b in the presence of the environmental noise

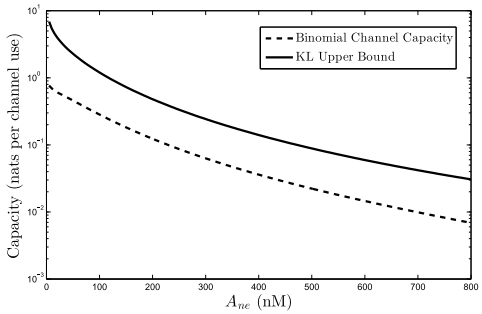

Fig. 6. Capacity and KL upper bound in terms of A_{ne} for the BIC with $A'_{\text{s}} = 80$, $N' = 20$, and $\alpha_{\text{s}} = \frac{1}{2}$.

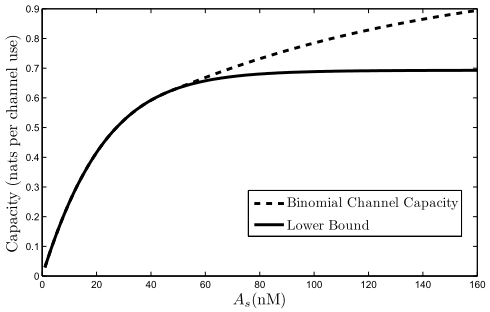

Fig. 7. Capacity and lower bound in terms of A'_{s} for the BIC with $N' = 20$ and $\alpha_{\text{s}} = \frac{1}{2}$.

$A_{\text{ne}}^{\text{LS}} = A_{\text{ne}}^{\text{TS}} = 5$. Fig. 5 shows the effect of blocking by showing the capacity of LS and TS for $m = 2$. As illustrated, the blocking decreases the capacity of TS. For small values of A_{s}, LS outperforms TS in all cases of blocking.

B. Lower Bound and KL Upper Bound on the Capacity of the Point-to-Point Channel

Our proposed KL upper bound, (18), and the capacity are depicted in Fig. 6 in the logarithmic scale. It can be observed that the distance between the KL upper bound and the capacity is constant in the logarithmic scale. Therefore, the gap between the capacity and the upper bound decreases as the environmental noise increases. The lower bound in (20) along with the capacity are shown in Fig. 7. For simplicity, we consider average constraint to be inactive. For small values of A'_{s}, our lower bound is tight which means the binary distribution is a capacity achieving distribution for small values of A'_{s}.

C. Multiple-Access Total Capacity

As mentioned in Section V, since there is no algorithm to compute the capacity region of the MAC numerically, we evaluate the total capacities of the DLSR and DMDR scenarios given in (32) and the SMSR scenario given in (33), using the extension of the BA algorithm for the total capacity of the MAC [35]. We assume $N = 10$, $n = 6$, and $m = 2$.

Fig. 8a shows the total capacities of the three scenarios in terms of $A_{\text{s},1} = A_{\text{s},2} = A_{\text{s}}$ when $A_{\text{ne}}^{\text{DLSR}} = A_{\text{ne}}^{\text{DMDR}} = A_{\text{ne}}^{\text{SMSR}} = 0$. It is observed that DLSR has the highest total capacity for all values of A_{s}. For small values of A_{s}, SMSR has higher total capacity than DMDR, whereas for large values of A_{s}, SMSR has lower total capacity than DMDR. The reason is that when A_{s} is small, sharing the receptors is useful. But when A_{s} increases, using different molecule types becomes more useful. Since DLSR has both of these advantages, it is more effective than the other two scenarios. Fig. 8b shows the total capacity for the three scenarios when $A_{\text{ne}}^{\text{DLSR}} = A_{\text{ne}}^{\text{DMDR}} = A_{\text{ne}}^{\text{SMSR}} = 5$. Similar conclusions can be made in the presence of the environmental noise.

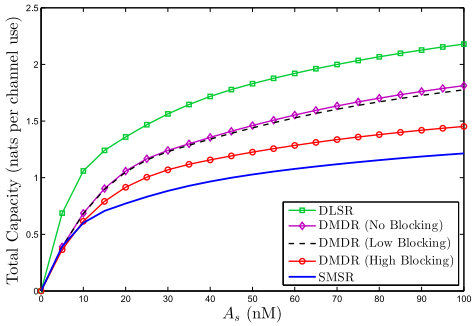

(a) $A_{\text{ne}}^{\text{DLSR}} = A_{\text{ne}}^{\text{DMDR}} = A_{\text{ne}}^{\text{SMSR}} = 0$

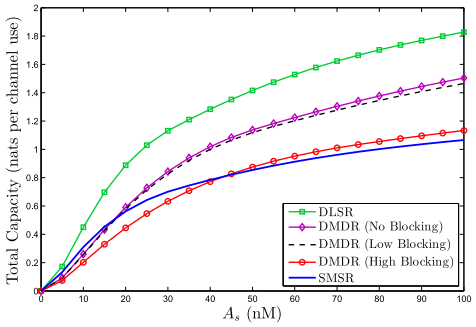

(b) $A_{\text{ne}}^{\text{DLSR}} = A_{\text{ne}}^{\text{DMDR}} = A_{\text{ne}}^{\text{SMSR}} = 5$

Fig. 8. Total capacity of DLSR, DMDR, and SMSR for $\alpha_{\text{s},1} = \alpha_{\text{s},2} = \frac{1}{2}$.

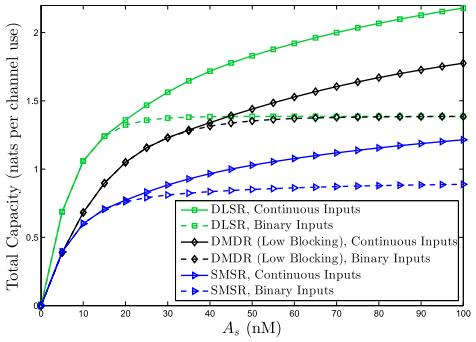

Fig. 9. Total capacity of DLSR, DMDR, and SMSR with continuous and binary inputs for $\alpha_{\text{s},1} = \alpha_{\text{s},2} = \frac{1}{2}$ and $A_{\text{ne}} = 0$.

Fig. 9 shows the effect of the binary input restriction on the total capacities of the three scenarios. It can be observed that in all three scenarios, the total capacities with binary inputs are equal to the total capacities with continuous inputs for small values of A_{s}. For large values of A_{s}, the total capacities of DLSR and DMDR with binary inputs reach to the same value since all receptors become full and these scenarios behave the same. However, the total capacity of SMSR with a

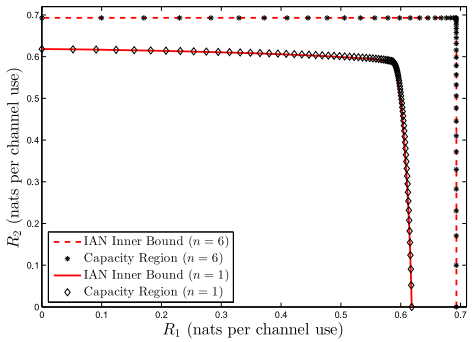

(a) DLSR

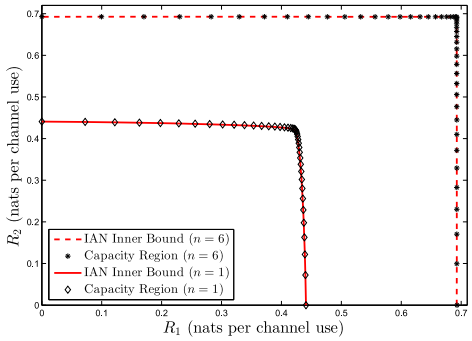

(b) DMDR with low blocking

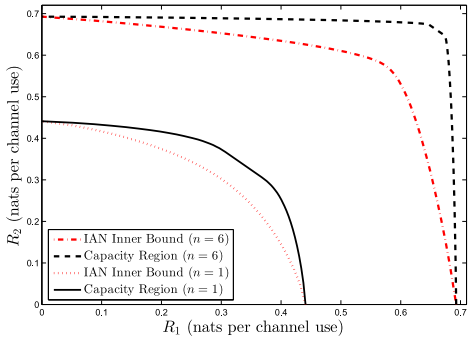

(c) DMDR with high blocking

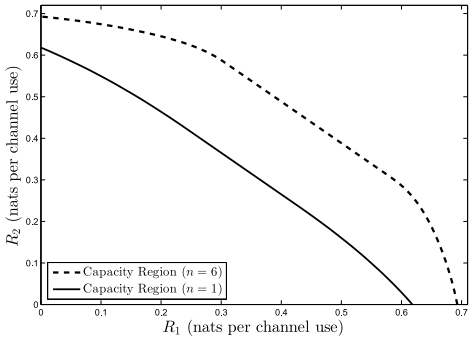

(d) SMSR

Fig. 10. Capacity region and Inner bounds for DLSR, DMDR, and SMSR with binary inputs for $A_{\mathrm{s},1} = A_{\mathrm{s},2} = 100$, $\alpha_{\mathrm{s},1} = \alpha_{\mathrm{s},2} = \frac{1}{2}$, and $A_{\mathrm{ne}} = 0$.

binary input reaches to a lower value since it doesn't have the advantage of using different molecule types or self-identifying labels.

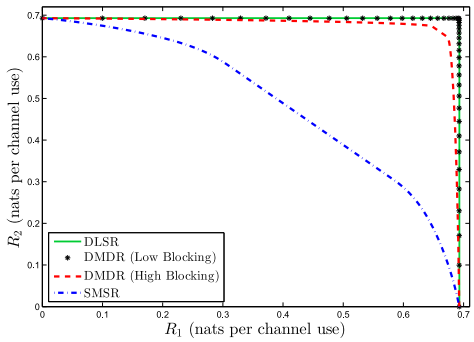

Fig. 11. Capacity region of DLSR, DMDR, and SMSR with binary inputs for $A_{\mathrm{s},1} = A_{\mathrm{s},2} = 100$, $\alpha_{\mathrm{s},1} = \alpha_{\mathrm{s},2} = \frac{1}{2}$, and $A_{\mathrm{ne}} = 0$.

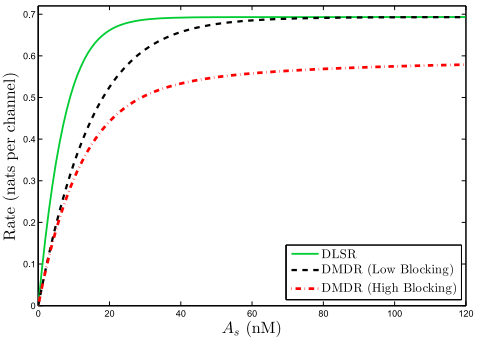

Fig. 12. Maximum achievable equal rates by viewing interference as noise for DLSR and DMDR with binary inputs for $\alpha_{\mathrm{s},1} = \alpha_{\mathrm{s},2} = \frac{1}{2}$ and $A_{\mathrm{ne}} = 0$.

D. Inner Bounds on the Capacity Region of the MAC

The IAN inner bounds for the DLSR and DMDR scenarios, provided in Section V-A, along with the capacity regions of the three scenarios with binary inputs are depicted in Fig. 10 for $N = 10$ and $n = 1, 6$. It is observed that in DMDR with low blocking and DLSR, the IAN inner bounds and the capacity regions are identical and when n increases, they become square-shaped, which indicates that these scenarios almost experience orthogonal MACs when n increases. In all scenarios, when n increases the maximum individual rates for the two transmitters increase and the capacity region with binary inputs becomes larger. The capacity regions of the three scenarios with binary inputs are shown in Fig. 11 for $N = 10$ and $n = 6$. It is observed that DMDR with low blocking and DLSR have the same square-shaped capacity regions. These two scenarios have the largest Capacity region and SMSR has the smallest capacity region and the capacity region of DMDR with high blocking is in middle.

Fig. 12 shows the maximum achievable equal rates of DMDR with low and high blocking and DLSR, given in (37), when considering interference as noise, in terms of $A_{\mathrm{s},1} = A_{\mathrm{s},2} = A_{\mathrm{s}}$ for $N = 10$ and $n = 6$. It is observed that the rate for DLSR is larger than DMDR and reaches to a constant value as A_{s} increases. Though the constant value is almost the same for DMDR with low blocking and DLSR, the value is higher than that of DMDR with high blocking. The reason is that when considering binary inputs and increasing A_{s}, DMDR with low blocking behaves like DLSR since all receptors become full. However, DMDR with high blocking

behaves worse than DLSR since some of the receptors are always blocked.

VII. Conclusion

In this paper, we first investigated the capacity performance of point-to-point communication scenarios, including Level and Type scenarios. We also modeled the blocking as a Markov process and derived the probabilities of binding and blocking. Next, we derived a new upper bound on the capacity of the BIC at low SNR-regime based on the KL divergence upper bound as well as a lower bound. As expected and confirmed by simulations, the blocking would decrease the capacity of the type scenario. Then we proposed three scenarios for the multiple-access communication, including the same molecule type with Different Labeling and Same Receptor type (DLSR), the Same Molecule type with the Same Receptor type (SMSR), and Different Molecule types with Different Receptor types (DMDR) scenarios and investigated their capacity region and total capacity. We derived some inner bounds on the capacity region of these scenarios when the environmental noise is negligible. Based on numerical results, DLSR outperforms the other scenarios for all values of the maximum signal level from the total capacity point of view. For small values of the maximum signal level, SMSR has better performance than DMDR, whereas DMDR has better performance for large values of maximum signal level.

Appendix A
Proof of Theorem 1

We find KL upper bound for the BIC as follows:

$$\begin{aligned}
I(X;Y) &\le \sum_{x,y}\big[P(x,y)-P(x)P(y)\big]\log P(y|x)\\
&= \sum_{x,y}\big[P(x,y)-P(x)P(y)\big]\\
&\quad\times\log\left(\binom{N'}{y}f_{p_{\mathrm{b}}}^{y}(x+A_{\mathrm{ne}})\big(1-f_{p_{\mathrm{b}}}(x+A_{\mathrm{ne}})\big)^{N'-y}\right)\\
&= \sum_{x}\left(\left(\sum_{y}yP(y|x)\right)\log\frac{f_{p_{\mathrm{b}}}(x+A_{\mathrm{ne}})}{1-f_{p_{\mathrm{b}}}(x+A_{\mathrm{ne}})}P(x)\right)\\
&\quad-\left(\sum_{x}\left(\sum_{y}yP(y|x)\right)P(x)\right)\\
&\quad\times\left(\sum_{x}\log\frac{f_{p_{\mathrm{b}}}(x+A_{\mathrm{ne}})}{1-f_{p_{\mathrm{b}}}(x+A_{\mathrm{ne}})}P(x)\right)\\
&= \mathbb{E}\left[N'f_{p_{\mathrm{b}}}(x+A_{\mathrm{ne}})\log\left(\frac{f_{p_{\mathrm{b}}}(x+A_{\mathrm{ne}})}{1-f_{p_{\mathrm{b}}}(x+A_{\mathrm{ne}})}\right)\right]\\
&\quad-\mathbb{E}\big[N'f_{p_{\mathrm{b}}}(x+A_{\mathrm{ne}})\big]\mathbb{E}\left[\log\left(\frac{f_{p_{\mathrm{b}}}(x+A_{\mathrm{ne}})}{1-f_{p_{\mathrm{b}}}(x+A_{\mathrm{ne}})}\right)\right]\\
&= N'\mathsf{Cov}\left(f_{p_{\mathrm{b}}}(X+A_{\mathrm{ne}}),\log\left(\frac{f_{p_{\mathrm{b}}}(X+A_{\mathrm{ne}})}{\big(1-f_{p_{\mathrm{b}}}(X+A_{\mathrm{ne}})\big)}\right)\right).
\end{aligned}$$

As mentioned earlier, $f_{p_{\mathrm{b}}}(X+A_{\mathrm{ne}})$ is an increasing function. Hence,

$$\mathsf{Cov}\left(f_{p_{\mathrm{b}}}(X+A_{\mathrm{ne}}),\log\left(\frac{f_{p_{\mathrm{b}}}(X+A_{\mathrm{ne}})}{\big(1-f_{p_{\mathrm{b}}}(X+A_{\mathrm{ne}})\big)}\right)\right)\ge 0.$$

A further observation is that $C\le\max_{P(x)}N'\mathsf{Cov}(f_{p_{\mathrm{b}}}(X+A_{\mathrm{ne}}),\log(\frac{f_{p_{\mathrm{b}}}(X+A_{\mathrm{ne}})}{(1-f_{p_{\mathrm{b}}}(X+A_{\mathrm{ne}}))}))$ is always achievable with a binary random variable X. We consider two points, x_1 and x_2 with probabilities p_1 and p_2, respectively. We have

$$\begin{aligned}
&\max_{P(x)}\mathsf{Cov}\big(f_{p_{\mathrm{b}}}(X+A_{\mathrm{ne}}),\log(F)\big)\\
&=\max_{\substack{P(x):\\F_1,F_2}}\big(\mathbb{E}\big[f_{p_{\mathrm{b}}}(X+A_{\mathrm{ne}})\log F\big]-\mathbb{E}\big[f_{p_{\mathrm{b}}}(X+A_{\mathrm{ne}})\big]\mathbb{E}\big[\log F\big]\big)\\
&=\max_{\substack{P(x):\\F1,F2}}\big(\mathbb{E}\big[\big(f_{p_{\mathrm{b}}}(X+A_{\mathrm{ne}})-\mathbb{E}\big[f_{p_{\mathrm{b}}}(X+A_{\mathrm{ne}})\big]\big)\log F\big]\big),
\end{aligned}$$

where $F=\frac{f_{p_{\mathrm{b}}}(X+A_{\mathrm{ne}})}{1-f_{p_{\mathrm{b}}}(X+A_{\mathrm{ne}})}$, $F1:\mathbb{E}(f_{p_{\mathrm{b}}}(X+A_{\mathrm{ne}}))\le\alpha_{\mathrm{s}}A'_{\mathrm{s}}$, and $F_2:0\le X\le A'_{\mathrm{s}}$. Now, based on the analysis in [16, Appendix C], the optimal distribution is given by $P(x)=\frac{\alpha_{\mathrm{s}}A'_{\mathrm{s}}}{f_{p_{\mathrm{b}}}(A'_{\mathrm{s}}+A_{\mathrm{ne}})}\delta(x-A'_{\mathrm{s}})+(1-\frac{\alpha_{\mathrm{s}}A'_{\mathrm{s}}}{f_{p_{\mathrm{b}}}(A'_{\mathrm{s}}+A_{\mathrm{ne}})})\delta(x)$ and the upper bound is obtained as

$$\max_{\alpha_{\mathrm{s}}A'_{\mathrm{s}}\le f_{p_{\mathrm{b}}}(\alpha_{\mathrm{s}}A'_{\mathrm{s}}+A_{\mathrm{ne}})}\frac{\alpha_{\mathrm{s}}A'_{\mathrm{s}}}{f_{p_{\mathrm{b}}}\big(A'_{\mathrm{s}}+A_{\mathrm{ne}}\big)}\big[f_{p_{\mathrm{b}}}\big(A'_{\mathrm{s}}+A_{\mathrm{ne}}\big)-\alpha_{\mathrm{s}}A'_{\mathrm{s}}\big]E,$$

where $E=\log(\frac{f_{p_{\mathrm{b}}}(A'_{\mathrm{s}}+A_{\mathrm{ne}})(1-f_{p_{\mathrm{b}}}(A_{\mathrm{ne}}))}{f_{p_{\mathrm{b}}}(A_{\mathrm{ne}})(1-f_{p_{\mathrm{b}}}(A'_{\mathrm{s}}+A_{\mathrm{ne}}))})$. Now, the upper bound is:

$$\begin{aligned}
A_{\mathsf{Binomial}}(P(y|x)) &:= \max_{\substack{P(x),\\\mathbb{E}[X]=\alpha_{\mathrm{s}}A'_{\mathrm{s}},\\0\le X\le A'_{\mathrm{s}}}}\mathcal{U}(P(x,y))\\
&= N'\begin{cases}\dfrac{f_{p_{\mathrm{b}}}\big(\alpha_{\mathrm{s}}A'_{\mathrm{s}}+A_{\mathrm{ne}}\big)}{f_{p_{\mathrm{b}}}\big(A'_{\mathrm{s}}+A_{\mathrm{ne}}\big)}\times F\times E & \text{if } (*),\\ \dfrac{f_{p_{\mathrm{b}}}\big(A'_{\mathrm{s}}+A_{\mathrm{ne}}\big)}{4}\times E & \text{if } (**),\end{cases}
\end{aligned}$$

where $E=\log(\frac{f_{p_{\mathrm{b}}}(A'_{\mathrm{s}}+A_{\mathrm{ne}})(1-f_{p_{\mathrm{b}}}(A_{\mathrm{ne}}))}{f_{p_{\mathrm{b}}}(A_{\mathrm{ne}})(1-f_{p_{\mathrm{b}}}(A'_{\mathrm{s}}+A_{\mathrm{ne}}))})$, $F=[f_{p_{\mathrm{b}}}(A'_{s}+A_{\mathrm{ne}})-f_{p_{\mathrm{b}}}(\alpha_{\mathrm{s}}A'_{\mathrm{s}}+A_{\mathrm{ne}})]$, $(*):f_{p_{\mathrm{b}}}(\alpha_{\mathrm{s}}A'_{\mathrm{s}}+A_{\mathrm{ne}})<\frac{f_{p_{\mathrm{b}}}(A'_{\mathrm{s}}+A_{\mathrm{ne}})}{2}$, and $(**):f_{p_{\mathrm{b}}}(\alpha_{\mathrm{s}}A'_{\mathrm{s}}+A_{\mathrm{ne}})\ge\frac{f_{p_{\mathrm{b}}}(A'_{\mathrm{s}}+A_{\mathrm{ne}})}{2}$.

Appendix B
Proof of Lemma 1

Let $p_c=(1-p_{\mathrm{b}})^{N'}$ and $P_{y|x}=P(Y=y|X=x)$. The BIC transition probabilities by considering a binary input is characterized as $P_{0|0}=1$, $P_{y|0}=0$, $P_{y|A'_{\mathrm{s}}}=\binom{N'}{y}p_{\mathrm{b}}^{y}(1-p_{\mathrm{b}})^{N'-y}$, for $y=1,\ldots,N'$.

Assume $P(X=A'_{\mathrm{s}})=\alpha$. The average constraint results in $\alpha\le\alpha_{\mathrm{s}}$. The lower bound on the BIC capacity

without considering the average constraint could be derived as follows:

$$\begin{aligned}C &= \max_{\alpha} I(X;Y)\\ &= \max_{\alpha} H(Y) - P(X=0)H(Y|X=0)\\ &\quad - P\big(X=A'_{\mathrm{s}}\big)H\big(Y|X=A'_{\mathrm{s}}\big)\\ &= \max_{\alpha} -\sum_{y=1}^{N'} \alpha P_{y|A'_{\mathrm{s}}} \log\big(\alpha P_{y|A'_{\mathrm{s}}}\big) - (1-\alpha+\alpha p_c)\\ &\quad \times \log(1-\alpha+\alpha p_c) - \alpha H\big(Y|X=A'_{\mathrm{s}}\big)\\ &= \max_{\alpha} -\alpha(1-p_c)\log\alpha + \alpha p_c \log p_c\\ &\quad -(1-\alpha+\alpha p_c)\log(1-\alpha+\alpha p_c).\end{aligned}$$

Taking a derivative with respect to α from $I(X;Y)$ and setting it to zero we obtain $\alpha^* = \frac{1}{1-p_c+e^{\frac{-p_c\log p_c}{1-p_c}}}$. Then, $C = H(\frac{1}{1+e^{g(p_c)}}) - \frac{g(p_c)}{1+e^{g(p_c)}}$. Now, if we consider the average constraint, the equation for C is valid for $\alpha^* \le \alpha_{\mathrm{s}}$ since the mutual information is concave in α. But for $\alpha^* > \alpha_{\mathrm{s}}$, the capacity lower bound is obtained for $\alpha = \alpha_{\mathrm{s}}$.

Appendix C
Proof of Lemma 2

We prove the lemma for the DLSR scenario. The approach for the DMDR scenario is the same. Let $p_{\mathrm{b},11} = p_{\mathrm{b},1}^{\mathrm{DLSR}}(X_1 = A_{\mathrm{s},1}, X_2 = x_2)$, $p_{\mathrm{b},21} = p_{\mathrm{b},2}^{\mathrm{DLSR}}(X_1 = A_{\mathrm{s},1}, X_2 = x_2)$, $P^1_{y_1|x_1,x_2} = P(Y_1 = y_1|X_1 = x_1, X_2 = x_2)$, $p_{c_1} = P^1_{0|A_{\mathrm{s},1},x_2} = (\frac{x_2+\frac{\kappa}{\gamma}}{A_{\mathrm{s},1}+x_2+\frac{\kappa}{\gamma}})^{nN}$, $p_{c_{10}} = P^1_{0|A_{\mathrm{s},1},0} = (\frac{\frac{\kappa}{\gamma}}{A_{\mathrm{s},1}+\frac{\kappa}{\gamma}})^{nN}$. Channel transition probabilities for the first transmitter by considering binary inputs $X_1 \in \{0, A_{\mathrm{s},1}\}$ and $X_2 \in \{0, A_{\mathrm{s},2}\}$ are characterized as $P^1_{0|0,x_2} = 1$ and $P^1_{y_1|A_{\mathrm{s},1},x_2} = \sum_{j=0}^{nN-y_1} \binom{nN}{y_1}\binom{nN-y_1}{j} p_{\mathrm{b},11}^{y_1} p_{\mathrm{b},21}^{j} (1-(p_{\mathrm{b},11}+p_{\mathrm{b},21}))^{nN-y_1-j}$, $\quad y_1 = 0,\ldots,nN$.

Assume $P(X_1 = A_{\mathrm{s},1}) = \alpha_1$. The average constraint for the first transmitter results in $\alpha_1 \le \alpha_{\mathrm{s},1}$. In the following, the maximum achievable individual rate for the first transmitter, C_1, is computed. The approach for computing C_2 is the same. Without considering the average constraint we have

$$\begin{aligned}C_1 &= \max_{x_2,\ \alpha_1} I(X_1;Y_1|X_2=x_2)\\ &= \max_{x_2,\ \alpha_1} H(Y_1|X_2=x_2)\\ &\quad - P(X_1=0)H(Y_1|X_1=0,X_2=x_2)\\ &\quad - P\big(X_1=A_{\mathrm{s},1}\big)H\big(Y_1|X_1=A_{\mathrm{s},1},X_2=x_2\big)\\ &\quad - \big(1-\alpha_1+\alpha_1 p_{c_1}\big)\log\big(1-\alpha_1+\alpha_1 p_{c_1}\big)\\ &\quad - \alpha_1 H\big(Y_1|X_1=A_{\mathrm{s},1},X_2=x_2\big)\\ &= \max_{x_2,\ \alpha_1} -\alpha_1\big(1-p_{c_1}\big)\log\alpha_1 + \alpha_1 p_{c_1}\log p_{c_1}\\ &\quad - \big(1-\alpha_1+\alpha_1 p_{c_1}\big)\log\big(1-\alpha_1+\alpha_1 p_{c_1}\big).\end{aligned}$$

Taking a derivative with respect to α_1 from $I(X_1;Y_1|X_2=x_2)$ and setting it to zero we obtain $\alpha_1^* = \frac{1}{1-p_{c_1}+e^{\frac{-p_{c_1}\log p_{c_1}}{1-p_{c_1}}}}$. Then, $C_1 = \max_{x_2}(H(\frac{1}{1+e^{g(p_{c_1})}}) - \frac{g(p_{c_1})}{1+e^{g(p_{c_1})}})$. Taking a derivative with respect to x_2 from $I_{\alpha_1^*}(X_1;Y_1|X_2=x_2)$ we obtain

$$\begin{aligned}&\frac{d}{dx_2} I_{\alpha_1^*}(X_1;Y|X_2=x_2)\\ &\quad = -\frac{p'_{c_1} g'\big(p_{c_1}\big) e^{g(p_{c_1})}}{\Big(1+e^{g(p_{c_1})}\Big)^2} H'\left(\frac{1}{1+e^{g(p_{c_1})}}\right)\\ &\qquad - \frac{p'_{c_1} g'\big(p_{c_1}\big)\Big(1+e^{g(p_{c_1})} - g\big(p_{c_1}\big)e^{g(p_{c_1})}\Big)}{\Big(1+e^{g(p_{c_1})}\Big)^2}.\end{aligned}$$

Since $H'(p) = \log(\frac{1-p}{p})$, we have

$$\begin{aligned}&\frac{d}{dx_2} I_{\alpha_1^*}(X_1;Y|X_2=x_2)\\ &= -\frac{p'_{c_1} g'\big(p_{c_1}\big)\Big(g\big(p_{c_1}\big)e^{g(p_{c_1})} + 1 + e^{g(p_{c_1})} - g\big(p_{c_1}\big)e^{g(p_{c_1})}\Big)}{\Big(1+e^{g(p_{c_1})}\Big)^2}\\ &= -\frac{p'_{c_1} g'\big(p_{c_1}\big)\Big(1+e^{g(p_{c_1})}\Big)}{\Big(1+e^{g(p_{c_1})}\Big)^2},\end{aligned}$$

and this is a negative value for all $x_2 \ge 0$ since $p'_{c_1} = \frac{nNA_{\mathrm{s},1}}{A_{\mathrm{s},1}+x_2+\frac{\kappa}{\gamma}}(\frac{x_2+\frac{\kappa}{\gamma}}{A_{\mathrm{s},1}+x_2+\frac{\kappa}{\gamma}})^{nN-1} > 0$ and $g'(p_{c_1}) = -\frac{p'_{c_1}\log p_{c_1}}{(1+e^{g(p_{c_1})})^2} > 0$. x_2 can take two values 0 and $A_{\mathrm{s},2}$. So the maximum occurs when $x_2 = 0$. Hence,

$$C_1 = H\left(\frac{1}{1+e^{g(p_{c_{10}})}}\right) - \frac{g\big(p_{c_{10}}\big)}{1+e^{g(p_{c_{10}})}}.$$

Now, we consider the average constraint. For both values of $x_2 = 0$ and $x_2 = A_{\mathrm{s},2}$, if $\alpha_{\mathrm{s},1} \ge \alpha_1^*(x_2)$, the maximum for $I(X_1;Y_1|X_2=x_2)$ occurs when $\alpha_1 = \alpha_1^*(x_2)$ and if $0 < \alpha_{\mathrm{s},1} < \alpha_1^*(x_2)$, the maximum occurs when $\alpha_1 = \alpha_{\mathrm{s},1}$ since $I(X_1,Y_1|X_2=x_2)$ is concave in α_1. Let $\alpha_{10}^* = \alpha_1^*(x_2=0)$ and $\alpha_{11}^* = \alpha_1^*(X_2 = A_{\mathrm{s},2})$. If $\alpha_{\mathrm{s},1} \ge \alpha_{10}^*$ and $\alpha_{\mathrm{s},1} \ge \alpha_{11}^*$, $C_1 = \max\{I_{\alpha_{10}^*}(X_1;Y_1|X_2=0), I_{\alpha_{11}^*}(X_1;Y_1|X_2=A_{\mathrm{s},2})\}$ equals to $I_{\alpha_{10}^*}(X_1;Y_1|X_2=0)$. If $\alpha_{\mathrm{s},1} \ge \alpha_{10}^*$ and $\alpha_{\mathrm{s},1} < \alpha_{11}^*$, $C_1 = \max\{I_{\alpha_{10}^*}(X_1;Y_1|X_2=0), I_{\alpha_{\mathrm{s},1}}(X_1;Y_1|X_2=As_2)\}$ equals to $I_{\alpha_{10}^*}(X_1;Y_1|X_2=0)$ since $I_{\alpha_{10}^*}(X_1;Y_1|X_2=0) > I_{\alpha_{11}^*}(X_1;Y_1|X_2=A_{\mathrm{s},2}) \ge I_{\alpha_{\mathrm{s},1}}(X_1;Y_1|X_2=A_{\mathrm{s},2})$. If $0 < \alpha_{\mathrm{s},1} < \alpha_{10}^*$ and $0 < \alpha_{\mathrm{s},1} < \alpha_{11}^*$, $C_1 = \max\{I_{\alpha_{\mathrm{s},1}}(X_1;Y_1|X_2=0), I_{\alpha_{\mathrm{s},1}}(X_1;Y_1|X_2=A_{\mathrm{s},2})\}$ equals to $I_{\alpha_{\mathrm{s},1}}(X_1;Y_1|X_2=0)$ since

$$\frac{d}{dx_2} I(X_1;Y|X_2=x_2) = \alpha_1 p'_{c_1}\log\frac{\alpha_1 p_{c_1}}{1-\alpha_1+\alpha_1 p_{c_1}} \le 0$$

and $I(X_1;Y_1|X_2=x_2)$ is a decreasing function with respect to x_2 for all values of $\alpha_1 \in [0,1]$. If $0 < \alpha_{\mathrm{s},1} < \alpha_{10}^*$ and $\alpha_{\mathrm{s},1} \ge \alpha_{11}^*$, $C_1 = \max\{I_{\alpha_{\mathrm{s},1}}(X_1;Y_1|X_2=0), I_{\alpha_{11}^*}(X_1;Y_1|X_2=A_{\mathrm{s},2})\}$ equals to $I_{\alpha_{\mathrm{s},1}}(X_1;Y_1|X_2=0)$ since $I_{\alpha_{\mathrm{s},1}}(X_1;Y_1|X_2=0) > I_{\alpha_{11}^*}(X_1;Y_1|X_2=0) > I_{\alpha_{11}^*}(X_1;Y_1|X_2=A_{\mathrm{s},2})$.

Appendix D
Proof of Lemma 3

We prove the lemma for the DLSR scenario. The approach for the DMDR scenario is the same. Let $p_{\mathrm{b},11} = p_{\mathrm{b},1}^{\mathrm{DLSR}}(X_1 =$

$A_{\mathrm{s},1}, X_2 = x_2)$, $p_{\mathrm{b},21} = p_{\mathrm{b},2}^{\mathrm{DLSR}}(X_1 = A_{\mathrm{s},1}, X_2 = x_2)$, $p_{\mathrm{b},12} = p_{\mathrm{b},1}^{\mathrm{DLSR}}(X_1 = x_1, X_2 = A_{\mathrm{s},2})$, $p_{\mathrm{b},22} = p_{\mathrm{b},2}^{\mathrm{DLSR}}(X_1 = x_1, X_2 = A_{\mathrm{s},2})$, $P^1_{y_1|x_1,x_2} = P(Y_1 = y_1|X_1 = x_1, X_2 = x_2)$, $P^2_{y_2|x_1,x_2} = P(Y_2 = y_2|X_1 = x_1, X_2 = x_2)$, $p_{c_{10}} = P^1_{0|A_{\mathrm{s},1},0} = (\frac{\frac{\kappa}{\gamma}}{A_{\mathrm{s},1}+\frac{\kappa}{\gamma}})^{nN}$, and $p_{c_{11}} = P^1_{0|A_{\mathrm{s},1},A_{\mathrm{s},2}} = (\frac{A_{\mathrm{s},2}+\frac{\kappa}{\gamma}}{A_{\mathrm{s},i}+A_{\mathrm{s},j}+\frac{\kappa}{\gamma}})^{nN}$.

Channel transition probabilities by considering binary inputs $x_1 \in \{0, A_{\mathrm{s},1}\}$ and $x_2 \in \{0, A_{\mathrm{s},2}\}$ are characterized as

$$P^1_{0|0,x_2} = P^2_{0|x_1,0} = 1,$$

$$P^1_{y_1|A_{\mathrm{s},1},x_2} = \sum_{j=0}^{nN-y_1} \binom{nN}{y_1}\binom{nN-y_1}{j} p_{\mathrm{b},11}^{y_1} p_{\mathrm{b},21}^{j} \times \big(1-\big(p_{\mathrm{b},11}+p_{\mathrm{b},21}\big)\big)^{nN-y_1-j},\ y_1 = 0,\ldots,nN,$$

$$P^2_{y_2|x_1,A_{\mathrm{s},2}} = \sum_{j=0}^{nN-y_2} \binom{nN}{y_2}\binom{nN-y_2}{j} p_{\mathrm{b},12}^{j} p_{\mathrm{b},22}^{y_2} \times \big(1-\big(p_{\mathrm{b},12}+p_{\mathrm{b},22}\big)\big)^{nN-y_2-j},\ y_2 = 0,\ldots,nN.$$

Assume $P(X_1 = A_{\mathrm{s},1}) = \alpha_1$ and $P(X_2 = A_{\mathrm{s},2}) = \alpha_2$. The average constraints result in $\alpha_1 \le \alpha_{\mathrm{s},1}$ and $\alpha_2 \le \alpha_{\mathrm{s},2}$. The IAN inner bound for this channel is computed as follows:

$$\begin{aligned}
R_1 &< I(X_1;Y_1) = H(Y_1) - P(X_1=0)H(Y_1|X_1=0) \\
&\quad - P\big(X_1=A_{\mathrm{s},1}\big)H\big(Y_1|X_1=A_{\mathrm{s},1}\big) \\
&= -\sum_{i=1}^{nN}\Big(\alpha_1\Big((1-\alpha_2)P^1_{y_1|A_{\mathrm{s},1},0} + \alpha_2 P^1_{y_1|A_{\mathrm{s},1},A_{\mathrm{s},2}}\Big)\Big) \\
&\quad \times \log\Big(\alpha_1\Big((1-\alpha_2)P^1_{y_1|A_{\mathrm{s},1},0} + \alpha_2 P^1_{y_1|A_{\mathrm{s},1},A_{\mathrm{s},2}}\Big)\Big) \\
&\quad - \big((1-\alpha_2)\big(1-\alpha_1+\alpha_1 p_{c_{10}}\big) + \alpha_2\big(1-\alpha_1+\alpha_1 p_{c_{11}}\big)\big) \\
&\quad \times \log\big((1-\alpha_2)\big(1-\alpha_1+\alpha_1 p_{c_{10}}\big) \\
&\quad + \alpha_2\big(1-\alpha_1+\alpha_1 p_{c_{11}}\big)\big) - \alpha_1 H\big(Y_1|X_1=A_{\mathrm{s},1}\big) \\
&= -\alpha_1\log\alpha_1 \sum_{i=1}^{nN}\Big((1-\alpha_2)P^1_{y_1|A_{\mathrm{s},1},0} + \alpha_2 P^1_{y_1|A_{\mathrm{s},1},A_{\mathrm{s},2}}\Big) \\
&\quad + \alpha_1\big(H\big(Y_1|X_1=A_{\mathrm{s},1}\big) + \big((1-\alpha_2)p_{c_{10}} + \alpha_2 p_{c_{11}}\big) \\
&\quad \times \log\big((1-\alpha_2)p_{c_{10}} + \alpha_2 p_{c_{11}}\big)\big) \\
&\quad - \big((1-\alpha_1) + \alpha_1\big((1-\alpha_2)p_{c_{10}} + \alpha_2 p_{c_{11}}\big)\big) \\
&\quad \times \log\big((1-\alpha_1) + \alpha_1\big((1-\alpha_2)p_{c_{10}} + \alpha_2 p_{c_{11}}\big)\big) \\
&\quad - \alpha_1 H\big(Y_1|x_1=A_{\mathrm{s},1}\big) \\
&= -\log\alpha_1 + \alpha_1\big((1-\alpha_2)p_{c_{10}} + \alpha_2 p_{c_{11}}\big) \\
&\quad \times \log\big((1-\alpha_2)p_{c_{10}} + \alpha_2 p_{c_{11}}\big) \\
&\quad - \alpha_1\left(\frac{1-\alpha_1}{\alpha_1} + (1-\alpha_2)p_{c_{10}} + \alpha_2 p_{c_{11}}\right) \\
&\quad \times \log\left(\frac{1-\alpha_1}{\alpha_1} + (1-\alpha_2)p_{c_{10}} + \alpha_2 p_{c_{11}}\right).
\end{aligned}$$

for some $\alpha_1 \in [0, \alpha_{\mathrm{s},1}]$ and $\alpha_2 \in [0, \alpha_{\mathrm{s},2}]$. With the same approach for R_2 we have

$$\begin{aligned}
R_2 &< -\log\alpha_2 + \alpha_2\big((1-\alpha_1)p_{c_{20}} + \alpha_1 p_{c_{21}}\big) \\
&\quad \times \log\big((1-\alpha_1)p_{c_{20}} + \alpha_1 p_{c_{21}}\big) \\
&\quad - \alpha_2\left(\frac{1-\alpha_2}{\alpha_2} + (1-\alpha_1)p_{c_{20}} + \alpha_1 p_{c_{21}}\right) \\
&\quad \times \log\left(\frac{1-\alpha_2}{\alpha_2} + (1-\alpha_1)p_{c_{20}} + \alpha_1 p_{c_{21}}\right).
\end{aligned}$$

For $A_{\mathrm{s},1} = A_{\mathrm{s},2} = A_{\mathrm{s}}$, we have $p_{c_{10}} = p_{c_{20}}$ and $p_{c_{11}} = p_{c_{21}}$. The points where $R_1 = R_2$ are obtained when $\alpha_1 = \alpha_2 = \alpha$ and without considering the average constraints, are as follows:

$$\begin{aligned}
R_1 = R_2 &= k\max_{\alpha} I(X_1;Y_1)|_{\alpha_1=\alpha_2=\alpha} \\
&= k\max_{\alpha} -\log\alpha + \alpha\big((1-\alpha)p_{c_{10}} + \alpha p_{c_{11}}\big) \\
&\quad \times \log\big((1-\alpha)p_{c_{10}} + \alpha p_{c_{11}}\big) \\
&\quad - \alpha\left(\frac{1-\alpha}{\alpha} + (1-\alpha)p_{c_{10}} + \alpha p_{c_{11}}\right) \\
&\quad \times \log\left(\frac{1-\alpha}{\alpha} + (1-\alpha)p_{c_{10}} + \alpha p_{c_{11}}\right),
\end{aligned}$$

for some $k \in [0, 1]$. Taking a derivative with respect to α from $I(X_1;Y_1)|_{\alpha_1=\alpha_2=\alpha}$ and setting it to zero we obtain

$$\begin{aligned}
&\big((1-2\alpha)p_{c_{10}} + 2\alpha p_{c_{11}}\big)\log\big((1-\alpha)p_{c_{10}} + \alpha p_{c_{11}}\big) \\
&\quad - \big((1-2\alpha)p_{c_{10}} + 2\alpha p_{c_{11}} - 1\big) \\
&\quad \times \log\left(\frac{1-\alpha}{\alpha} + (1-\alpha)p_{c_{10}} + \alpha p_{c_{11}}\right) = 0.
\end{aligned}$$

If we consider the average constraints with $\alpha_{\mathrm{s},1} = \alpha_{\mathrm{s},2} = \alpha_{\mathrm{s}}$, the above equation for the optimum value of α is valid if the solution of the equation is lower than or equal to α_{s} since $I(X_1;Y_1)$ for $\alpha_1 = \alpha_2 = \alpha$ is concave in α. If the solution is higher than α_{s}, the maximum occurs when $\alpha = \alpha_{\mathrm{s}}$.

APPENDIX E
PROOF OF LEMMA 4

Let $p_{\mathrm{b},10} = p_{\mathrm{b}}^{\mathrm{SMSR}}(X_1 = A_{\mathrm{s},1}, X_2 = 0)$, $p_{\mathrm{b},01} = p_{\mathrm{b}}^{\mathrm{SMSR}}(X_1 = 0, X_2 = A_{\mathrm{s},2})$, $p_{\mathrm{b},11} = p_{\mathrm{b}}^{\mathrm{SMSR}}(X_1 = A_{\mathrm{s},1}, X_2 = A_{\mathrm{s},2})$, $P_{y|x_1,x_2} = P(Y = y|X_1 = x_1, X_2 = x_2)$, and $p_{c_{10}} = P_{y|A_{\mathrm{s},1},0} = (\frac{\frac{\kappa}{\gamma}}{A_{\mathrm{s},1}+\frac{\kappa}{\gamma}})^{nN}$.

Channel transition probabilities by considering binary inputs $X_1 \in \{0, A_{\mathrm{s},1}\}$ and $X_2 \in \{0, A_{\mathrm{s},2}\}$ are characterized as $P_{0|0,0} = 1$, $P_{y|A_{\mathrm{s},1},0} = \binom{nN}{y} p_{\mathrm{b},10}^{y}(1-p_{\mathrm{b},10})^{nN-y}$ $P_{y|0,A_{\mathrm{s},2}} = \binom{nN}{y} p_{\mathrm{b},01}^{y}(1-p_{\mathrm{b},01})^{nN-y}$ and $P_{y|A_{\mathrm{s},1},A_{\mathrm{s},2}} = \binom{nN}{y} p_{\mathrm{b},11}^{y}(1-p_{\mathrm{b},01})^{nN-y}$ for $y = 0,\ldots,nN$. Assume $P(X_1 = A_{\mathrm{s},1}) = \alpha_1$. The average constraint for the first transmitter results in $\alpha_1 \le \alpha_{\mathrm{s},1}$. In the following, the maximum achievable individual rate for the first transmitter, C_1, is computed. The approach for computing C_2 is the same. Without considering the average constraint we have

$$\begin{aligned}
C_1 &= \max_{x_2,\ \alpha_1} I(X_1;Y|X_2=x_2) \\
&= \max_{x_2,\ \alpha_1} H(Y|X_2=x_2) \\
&\quad - P(X_1=0)H(Y|X_1=0,X_2=x_2) \\
&\quad - P\big(X_1=A_{\mathrm{s},1}\big)H\big(Y|X_1=A_{\mathrm{s},1},X_2=x_2\big) \\
&= \max_{x_2,\ \alpha_1} -\sum_{y=0}^{nN} P(Y=y|X_2=x_2)\log P(Y=y|X_2=x_2) \\
&\quad - (1-\alpha_1)H(Y|X_1=0,X_2=x_2) \\
&\quad - \alpha_1 H\big(Y|X_1=A_{\mathrm{s},1},X_2=x_2\big).
\end{aligned}$$

We can write this as $C_1 = \max\{c_{10}, c_{11}\}$, $c_{10} = \max_{\alpha_1} I(X_1; Y|X_2 = 0)$, $c_{11} = \max_{\alpha_1} I(X_1; Y|X_2 = A_{\mathrm{s},2})$. For c_{10} we have

$$\begin{aligned} c_{10} &= \max_{\alpha_1} -\sum_{y=0}^{nN} P(Y=y|X_2=0)\log P(Y=y|X_2=0) \\ &\quad - \alpha_1 H\big(Y|X_1=A_{\mathrm{s},1}, X_2=0\big) \\ &= \max_{\alpha_1} -\alpha_1\big(1-p_{c_{10}}\big)\log\alpha_1 + \alpha_1 p_{c_{10}}\log p_{c_{10}} \\ &\quad - \big(1-\alpha_1+\alpha_1 p_{c_{10}}\big)\log\big(1-\alpha_1+\alpha_1 p_{c_{10}}\big). \end{aligned}$$

Taking a derivative with respect to α_1 from $I(X_1; Y|X_2 = 0)$ and setting it to zero we obtain $\alpha_{10}^* = \frac{1}{1-p_{c_{10}}+e^{-\frac{p_{c_{10}}\log p_{c_{10}}}{1-p_{c_{10}}}}}$, Then, $c_{10} = H(\frac{1}{1+e^{g(p_{c_{10}})}}) - \frac{g(p_{c_{10}})}{1+e^{g(p_{c_{10}})}}$. If we consider the average constraint, the above equation for c_{10} is valid if $\alpha_{\mathrm{s},1} \geq \alpha_{10}^*$ since $I(X_1; Y_1|X_2 = 0)$ is concave in α_1. If $0 < \alpha_{\mathrm{s},1} < \alpha_{10}^*$, the maximum occurs when $\alpha_1 = \alpha_{\mathrm{s},1}$. For c_{11} we have

$$\begin{aligned} c_{11} &= \max_{\alpha_1} I\big(X_1; Y|X_2=A_{\mathrm{s},2}\big) \\ &= \max_{\alpha_1} -\sum_{y=0}^{nN}\big((1-\alpha_1)P_{y|0,A_{\mathrm{s},2}} + \alpha_1 P_{y|A_{\mathrm{s},1},A_{\mathrm{s},2}}\big) \\ &\quad \times \log\big((1-\alpha_1)P_{y|0,A_{\mathrm{s},2}} + \alpha_1 P_{y|A_{\mathrm{s},1},A_{\mathrm{s},2}}\big) \\ &\quad - (1-\alpha_1)H\big(Y|X_1=0, X_2=A_{\mathrm{s},2}\big) \\ &\quad - \alpha_1 H\big(Y|X_1=A_{\mathrm{s},1}, X_2=A_{\mathrm{s},2}\big) \\ &= \max_{\alpha_1} -\sum_{y=0}^{nN}\Bigg[(1-\alpha_1)P_{y|0,A_{\mathrm{s},2}} \\ &\quad \times \log\left((1-\alpha_1)+\alpha_1\frac{P_{y|A_{\mathrm{s},1},A_{\mathrm{s},2}}}{P_{0,A_{\mathrm{s},2}}}\right) \\ &\quad + \alpha_1 P_{y|A_{\mathrm{s},1},A_{\mathrm{s},2}}\log\left((1-\alpha_1)\frac{P_{y|0,A_{\mathrm{s},2}}}{P_{y|A_{\mathrm{s},1},A_{\mathrm{s},2}}}+\alpha_1\right)\Bigg]. \end{aligned}$$

Taking a derivative with respect to α_1 from $I(X_1; Y|X_2 = A_{\mathrm{s},2})$ and setting it to zero we obtain

$$\begin{aligned} &\sum_{y=0}^{nN}\Bigg[P_{y|0,A_{\mathrm{s},2}}\log\left((1-\alpha_1)+\alpha_1\frac{P_{y|A_{\mathrm{s},1},A_{\mathrm{s},2}}}{P_{y|0,A_{\mathrm{s},2}}}\right) \\ &\qquad - P_{y|A_{\mathrm{s},1},A_{\mathrm{s},2}}\log\left((1-\alpha_1)\frac{P_{y|0,A_{\mathrm{s},2}}}{P_{y|A_{\mathrm{s},1},A_{\mathrm{s},2}}}+\alpha_1\right)\Bigg] = 0. \end{aligned}$$

If we consider the average constraint, the above equation for the optimum value of α_1 is valid when the solution of the equation is lower than or equal to $\alpha_{\mathrm{s},1}$ since $I(X_1; Y_1|X_2 = A_{\mathrm{s},2})$ is concave in α_1. If the solution is higher than $\alpha_{\mathrm{s},1}$, the maximum occurs when $\alpha_1 = \alpha_{\mathrm{s},1}$.

ACKNOWLEDGMENT

The authors would like to thank Dr. Amin Gohari for his helpful comments.

REFERENCES

[1] M. S. Kuran, H. B. Yilmaz, T. Tugcu, and I. F. Akyildiz, "Modulation techniques for communication via diffusion in nanonetworks," in *Proc. IEEE Int. Conf. Commun. (ICC)*, Kyoto, Japan, Jun. 2011, pp. 1–5.

[2] B. Tepekule, A. E. Pusane, H. B. Yilmaz, and T. Tugcu, "A novel modulation technique in diffusion based molecular communication and its performance analysis," in *Proc. 22nd Signal Process. Commun. Appl. Conf. SIU*, Trabzon, Turkey, Apr. 2014, pp. 1110–1113.

[3] D. Arifler, "Capacity analysis of a diffusion-based short-range molecular nano-communication channel," *Comput. Netw.*, vol. 55, no. 6, pp. 1426–1434, 2011.

[4] A. Einolghozati, M. Sardari, and F. Fekri, "Capacity of diffusion-based molecular communication with ligand receptors," in *Proc. IEEE Inf. Theory Workshop (ITW)*, Paraty, Brazil, Oct. 2011, pp. 85–89.

[5] B. Atakan, *Molecular Communication Among Nanomachines*. New York, NY, USA: Springer, 2014.

[6] G. Alfano and D. Miorandi, "On information transmission among nanomachines," in *Proc. IEEE ICST 1st Int. Conf. Nano-Netw.*, Lausanne, Switzerland, Sep. 2006, pp. 1–5.

[7] A. W. Eckford, "Molecular communication: Physically realistic models and achievable information rates," *arXiv preprint arXiv:0812.1554*, 2008.

[8] K. V. Srinivas, A. W. Eckford, and R. S. Adve, "Molecular communication in fluid media: The additive inverse Gaussian noise channel," *IEEE Trans. Inf. Theory*, vol. 58, no. 7, pp. 4678–4692, Jul. 2012.

[9] H. Li, S. M. Moser, and D. Guo, "Capacity of the memoryless additive inverse Gaussian noise channel," *IEEE J. Sel. Areas Commun.*, vol. 32, no. 12, pp. 2315–2329, Dec. 2014.

[10] A. W. Eckford and P. J. Thomas, "Capacity of a simple intercellular signal transduction channel," in *Proc. IEEE Int. Symp. Inf. Theory*, Istanbul, Turkey, Jul. 2013, pp. 1834–1838.

[11] B. Atakan and O. B. Akan, "On channel capacity and error compensation in molecular communication," in *Transactions on Computational Systems Biology X*. Heidelberg, Germany: Springer, 2008, pp. 59–80.

[12] A. Einolghozati, M. Sardari, A. Beirami, and F. Fekri, "Capacity of discrete molecular diffusion channels," in *Proc. IEEE Int. Symp. Inf. Theory (ISIT)*, St. Petersburg, Russia, Jul./Aug. 2011, pp. 723–727.

[13] Q. Liu, K. Yang, and P. He, "Channel capacity analysis for molecular communication with continuous molecule emission," in *Proc. Int. Conf. Wireless Commun. Signal Process. (WCSP)*, Hangzhou, China, Oct. 2013, pp. 1–6.

[14] M. Ş. Kuran, H. B. Yilmaz, T. Tugcu, and I. F. Akyildiz, "Interference effects on modulation techniques in diffusion based nanonetworks," *Nano Commun. Netw.*, vol. 3, no. 1, pp. 65–73, 2012.

[15] M. Pierobon and I. F. Akyildiz, "Capacity of a diffusion-based molecular communication system with channel memory and molecular noise," *IEEE Trans. Inf. Theory*, vol. 59, no. 2, pp. 942–954, Feb. 2013.

[16] G. Aminian, H. Arjmandi, A. Gohari, M. Nasiri-Kenari, and U. Mitra, "Capacity of diffusion-based molecular communication networks over LTI-Poisson channels," *IEEE Trans. Mol. Biol. Multi-Scale Commun.*, vol. 1, no. 2, pp. 188–201, Jun. 2015.

[17] A. Einolghozati, M. Sardari, and F. Fekri, "Design and analysis of wireless communication systems using diffusion-based molecular communication among bacteria," *IEEE Trans. Wireless Commun.*, vol. 12, no. 12, pp. 6096–6105, Dec. 2013.

[18] M. Pierobon and I. F. Akyildiz, "Noise analysis in ligand-binding reception for molecular communication in nanonetworks," *IEEE Trans. Signal Process.*, vol. 59, no. 9, pp. 4168–4182, Sep. 2011.

[19] S. M. Moser, "Capacity results of an optical intensity channel with input-dependent Gaussian noise," *IEEE Trans. Inf. Theory*, vol. 58, no. 1, pp. 207–223, Jan. 2012.

[20] Q. Xie and A. R. Barron, "Minimax redundancy for the class of memoryless sources," *IEEE Trans. Inf. Theory*, vol. 43, no. 2, pp. 646–657, Mar. 1997.

[21] C. Komninakis, L. Vandenberghe, and R. D. Wesel, "Capacity of the binomial channel, or minimax redundancy for memoryless sources," in *Proc. IEEE Int. Symp. Inf. Theory (ISIT)*, Washington, DC, USA, 2001, p. 127.

[22] M. Tahmasbi and F. Fekri, "On the capacity achieving probability measures for molecular receivers," in *Proc. IEEE Inf. Theory Workshop-Fall (ITW)*, Jeju Island, South Korea, Oct. 2015, pp. 109–113.

[23] B. Tepekule, A. E. Pusane, H. B. Yilmaz, C.-B. Chae, and T. Tugcu, "ISI mitigation techniques in molecular communication," *IEEE Trans. Mol. Biol. Multi-Scale Commun.*, vol. 1, no. 2, pp. 202–216, Jun. 2015.

[24] D. Kilinc and O. B. Akan, "Receiver design for molecular communication," *IEEE J. Sel. Areas Commun.*, vol. 31, no. 12, pp. 705–714, Dec. 2013.

[25] A. Noel, K. C. Cheung, and R. Schober, "Improving receiver performance of diffusive molecular communication with enzymes," *IEEE Trans. Nanobiosci.*, vol. 13, no. 1, pp. 31–43, Mar. 2014.

[26] B. Atakan and O. B. Akan, "On molecular multiple-access, broadcast, and relay channels in nanonetworks," in *Proc. 3rd Int. Conf. Bio-Inspired Models Netw. Inf. Comput. Syst.*, Hyogo, Japan, 2008, p. 16.
[27] B. Atakan and O. B. Akan, "Single and multiple-access channel capacity in molecular nanonetworks," in *Nano-Net*. Heidelberg, Germany: Springer, 2009, pp. 14–23.
[28] Q. Liu and K. Yang, "Multiple-access channel capacity of diffusion and ligand-based molecular communication," in *Proc. 16th ACM Int. Conf. Model. Anal. Simulat. Wireless Mobile Syst. (MSWiM)*, Barcelona, Spain, Nov. 2013, pp. 151–158.
[29] M. A. Cooper, "Label-free screening of bio-molecular interactions," *Anal. Bioanal. Chem.*, vol. 377, no. 5, pp. 834–842, 2003.
[30] J. Müller, C. Kuttler, and B. A. Hense, "Sensitivity of the quorum sensing system is achieved by low pass filtering," *Biosystems*, vol. 92, no. 1, pp. 76–81, 2008.
[31] D. A. Lauffenburger and J. J. Linderman, *Receptors: Models for Binding, Trafficking, and Signaling*. New York, NY, USA: Oxford Univ. Press, 2011.
[32] A. A. El Gamal and Y.-H. Kim, *Network Information Theory*. Cambridge, U.K.: Cambridge Univ. Press, 2011.
[33] E. Calvo, D. P. Palomar, J. R. Fonollosa, and J. Vidal, "On the computation of the capacity region of the discrete MAC," *IEEE Trans. Commun.*, vol. 58, no. 12, pp. 3512–3525, Dec. 2010.
[34] R. Blahut, "Computation of channel capacity and rate-distortion functions," *IEEE Trans. Inf. Theory*, vol. 18, no. 4, pp. 460–473, Jul. 1972.
[35] M. Rezaeian and A. Grant, "Computation of total capacity for discrete memoryless multiple-access channels," *IEEE Trans. Inf. Theory*, vol. 50, no. 11, pp. 2779–2784, Nov. 2004.

Gholamali Aminian received the B.S. degree in electrical engineering from Amirkabir University, Tehran, Iran, in 2010, and the M.S. degree in electrical engineering from the Sharif University of Technology, Tehran, in 2012, where he is currently pursuing the Ph.D. degree in electrical. His field of interest includes nano communication, wireless communication, and information theory.

Maryam Farahnak-Ghazani received the B.S. degree in electrical engineering from the Sharif University of Technology, Tehran, Iran, in 2014, where she is currently pursuing the M.S. degree with the Department of Electrical Engineering. Her main research interests include nano-scale communication, molecular communication networks, wireless communication, and information theory.

Mahtab Mirmohseni (S'06–M'12) received the B.Sc., M.Sc., and Ph.D. degrees in communication systems from the Electrical Engineering Department, Sharif University of Technology (SUT), Tehran, Iran, in 2005, 2007, and 2012, respectively. She was a Post-Doctoral Researcher with the School of Electrical Engineering, Royal Institute of Technology, Stockholm, Sweden, until 2014. Since 2014, she has been an Assistant Professor with the Electrical Engineering Department, SUT. She is also affiliated with the Information Systems and Security Laboratory, SUT. Her current research interests include information theory of molecular communication, secure communication, and energy-constrained networks.

Masoumeh Nasiri-Kenari received the B.S. and M.S. degrees from the Isfahan University of Technology, Isfahan, Iran, in 1986 and 1987, respectively, and the Ph.D. degree from the University of Utah, Salt Lake City, in 1993, all in electrical engineering. From 1987 to 1988, she was a Technical Instructor and a Research Assistant with the Isfahan University of Technology. Since 1994, she has been with the Department of Electrical Engineering, Sharif University of Technology, Tehran, Iran, where she is currently a Professor.

Dr. Nasiri-Kenari founded the Wireless Research Laboratory, Electrical Engineering Department, in 2001, to coordinate the research activities in the field of wireless communication. From 1999 to 2001, she was the Co-Director of the Advanced Communication Research Laboratory, Iran Telecommunication Research Center, Tehran. Since 2014, she has been an Associate Editor of the IEEE TRANSACTIONS ON COMMUNICATIONS. She was a recipient of the Distinguished Researcher Award and the Distinguished Lecturer Award of the EE Department, Sharif University of Technology, in 2005 and 2007, respectively, the Research Chair on Nano Communication Networks from Iran National Science Foundation and the 2014 Premium Award for Best Paper in IET Communications. She holds a research grant on green communication in multirelay wireless networks for the years 2015–2017 from the Swedish Research Council.

Faramarz Fekri received the Ph.D. degree from the Georgia Institute of Technology, in 2000. Since 2000, he has been with the faculty of the School of Electrical and Computer Engineering, Georgia Institute of Technology, where he is currently a Professor. He serves on the technical program committees of several IEEE conferences. His current research interests are in the area of communications and signal processing, in particular source and channel coding, information theory in biology, statistical inference in large data, information processing for wireless and sensor networks, and communication security. He is an Associate Editor of the IEEE TRANSACTIONS ON MOLECULAR, BIOLOGICAL, AND MULTI-SCALE COMMUNICATIONS. He served on the Editorial Board of the IEEE TRANSACTIONS ON COMMUNICATIONS and the *Elsevier Journal on PHYCOM*. He was a recipient of the National Science Foundation CAREER Award in 2001, the Southern Center for Electrical Engineering Education Young Faculty Development Award in 2003, and the Outstanding Young Faculty Award of the School of ECE in 2006.